Recent Results from LEP at the Z on Electroweak and Heavy Flavour Physics

Klaus Mönig
CERN/PPE
1211 Genève 23
Switzerland

Abstract

The four LEP experiments ALEPH, DELPHI, L3 and OPAL have collected about four million Z decays each between 1990 and 1995 at energies close to the Z-pole. Most of the data have been taken between 1992 and 1995 on the peak and at approximately 2GeV above and below.
Recent preliminary results, using a large fraction of the full statistics, are presented on electroweak and selected topics of b-physics.

Invited talk given at the SLAC Summer Institute 1996

1   Introduction

Between 1989 and 1995 LEP has been operated at centre of mass energies of a few GeV around the Z-peak. Each experiment has collected about $4 \cdot 10^6$ hadronic and $4 \cdot 10^5$ leptonic Z-decays. Out of this the luminosity collected at energies few GeV away from the nominal Z-mass is about 40pb^{-1} per experiment.

Apart from the usual tracking and calorimetry all experiments are equipped with powerful silicon microvertex detectors allowing for an efficient tagging of b- and c-quarks.

For the determination of the Z resonance parameters close to the full statistics has been used. For most other analyses the data taken up to 1994 are included which corresponds to more than 80% of the total available statistics.

For all of the electroweak and for some important b-physics quantities the LEP collaborations have taken a special effort to combine the results in a consistent way, taking into account common systematic uncertainties.

2   The Z-lineshape

The cross section section $e^+e^- \rightarrow f\bar{f}$, $f \neq e$ near the Z-pole at a centre of mass energy $\sqrt{s}$ can be written as

$$\sigma_f(s) = \frac{12\pi}{m_Z} \frac{\Gamma_e \Gamma_f s}{(s - m_Z^2)^2 + \left(\frac{s}{m_Z}\right)^2 \Gamma_Z^2} + \sigma_\gamma + \sigma_{\text{int}} + \text{rad. cor.}$$

The first term describes the dominant contribution from Z exchange, σ_γ and σ_{int} denote the contributions from γ-exchange and $\gamma - Z$ interference which are very much suppressed at centre of mass energies close to the Z-mass. The radiative corrections can be calculated in QED and depend only on the cross section at energies below the centre of mass energy at which the cross section is measured. Γ_Z stands for the total decay width of the Z and Γ_f for its partial decay width into an $f\bar{f}$ pair. For $f = e$ in addition the contributions from t-channel γ and Z exchange have to be added.

The LEP experiments extract from the cross sections a set of minimal correlated parameters that are more convenient for averaging and for electroweak fits. These parameters are:

$$m_Z$$
$$\Gamma_Z$$
$$\sigma_0^{\text{had}} = \frac{12\pi}{m_Z} \frac{\Gamma_e \Gamma_{\text{had}}}{\Gamma_Z^2}$$
$$R_\ell = \frac{\Gamma_{\text{had}}}{\Gamma_\ell} \quad \ell = e, \mu, \tau$$

The maximum correlation between these parameters is 14%.

2.1   Determination of the beam energy

The determination of the Z mass and width depends crucially on the accurate knowledge of the LEP beam energy for the off-peak fills. For that reason at the end of each such fill an energy calibration using the resonant depolarization technique is attempted, which determines the beam energy to a precision of about 0.2MeV. However the total error on the beam energy is significantly larger for several reasons:

- Only a part of the off peak fills are successfully calibrated at the end (40% in 1993, 70% in 1995). For the the others an extrapolation model is needed.
- Imperfections in the RF system make the energies in the interaction points different from the mean energy. These errors are anticorrelated between the different experiments so that they cancel to a large extend in the LEP average.
- The beam energy rises with time due to hysteresis effects in the LEP magnets. This effect has been discovered only during the 1995 scan due to newly installed NMR probes in the LEP-tunnel. As illustrated in figure 1 these effects are originated by leakage currents through the beam pipe induced by trains in the Geneva region.

A detailed description of the full procedure can be found in [1]. The total error on the Z mass and width by the limited knowledge on the beam energy is $\Delta m_Z = 1.5\text{MeV}$ and $\Delta\Gamma_Z = 1.7\text{MeV}$.

2.2 Measurement of the cross section

Generally a cross section is given by

$$\sigma = \frac{N}{\mathcal{L}},$$

where N is the acceptance and background corrected number of events and $\mathcal{L}$ the integrated luminosity.

The large acceptance of the LEP detectors and the clean environment of the accelerator allow for a determination of the event rate of typically better than 0.1% for $e^+e^- \to$ hadrons and better than 0.5% for the leptonic channels.

The luminosity at LEP is determined from Bhabha scattering at low angles for which the cross section can be calculated reliably in QED. All experiments measure this cross section now to better than 0.1% and the theoretical calculation is accurate to 0.11%.

2.3 Results

The results on the Z-lineshape from the different experiments can be found in [2–5] and are summarized in table 1. As an example the hadronic lineshape measured by the L3 collaboration is shown in figure 2. Combining the four experiments yields:

$$
\begin{aligned}
m_Z &= 91.1863 \pm 0.0020\,\text{GeV} \\
\Gamma_Z &= 2.4946 \pm 0.0027\,\text{GeV} \\
\sigma_0^{\text{had}} &= 41.508 \pm 0.056\,\text{nb} \\
R_e &= 20.754 \pm 0.057 \\
R_\mu &= 20.796 \pm 0.040 \\
R_\tau &= 20.814 \pm 0.055 \\
R_\ell &= 20.778 \pm 0.029
\end{aligned}
$$

where R_ℓ is the result assuming lepton universality corrected to a massless lepton. From this the following partial widths can be derived:

$$
\begin{aligned}
\Gamma_{\text{had}} &= 1743.6 \pm 2.5\,\text{MeV} \\
\Gamma_e &= 83.96 \pm 0.15\,\text{MeV} \\
\Gamma_\mu &= 83.79 \pm 0.22\,\text{MeV} \\
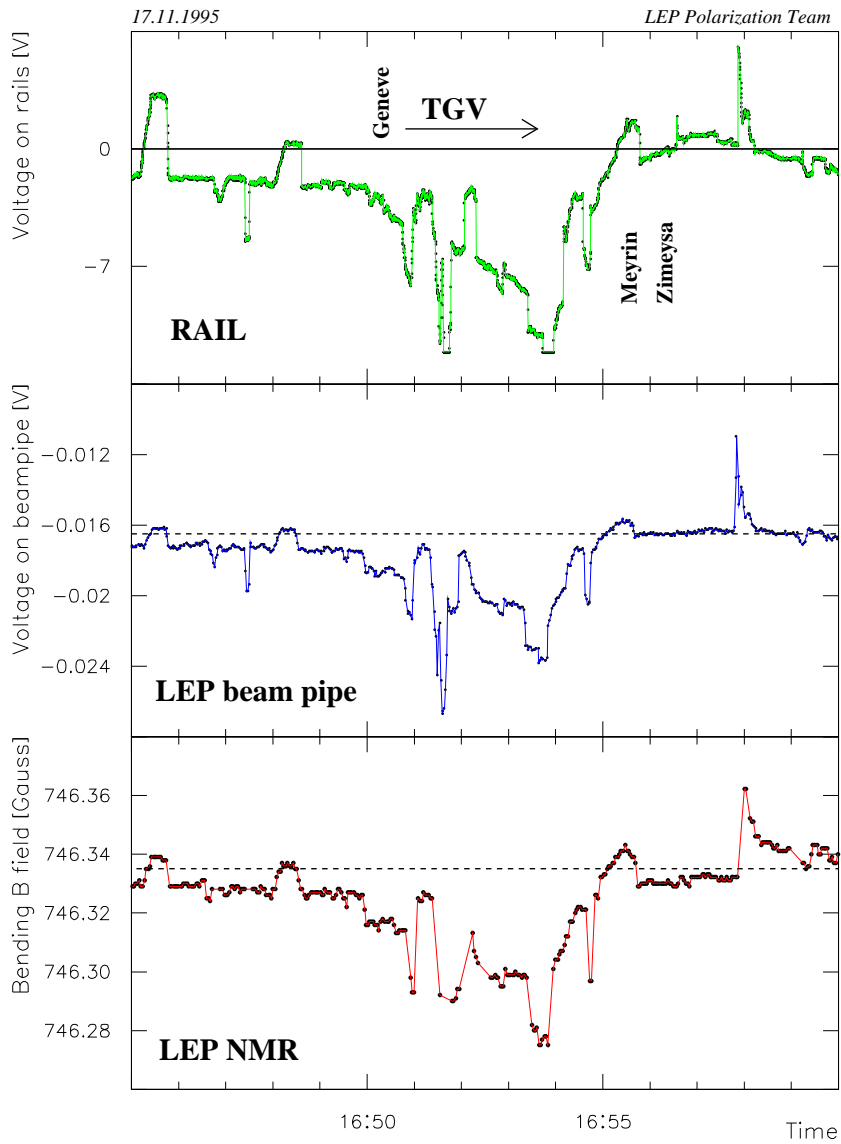\Gamma_\tau &= 83.72 \pm 0.26\,\text{MeV}
\end{aligned}
$$

2

Figure 1: Effect of trains on the LEP beam energy. The upper plot shows the voltage measured on the rails while a train is passing close to the LEP tunnel. The middle plot shows the voltage measured simultaneously on the LEP beam pipe and the lower plot the field of the dipole magnets measured by an NMR probe.

3

$$\Gamma_\ell = 83.91 \pm 0.11 \, \text{MeV}$$
$$\Gamma_{inv.} = 499.5 \pm 2.0 \, \text{MeV}$$

Taking the ratio of the leptonic to the neutrino partial width from the Standard Model yields for the number of light neutrino generations:

$$N_\nu = 2.989 \pm 0.012.$$

	ALEPH	DELPHI	L3	OPAL
$m_{\rm Z}(\text{GeV})$	91.1873±0.0030	91.1859±0.0028	91.1883±0.0029	91.1824±0.0039
$\Gamma_{\rm Z}(\text{GeV})$	2.4950±0.0047	2.4896±0.0042	2.4996±0.0043	2.4956±0.0053
$\sigma_0^{\rm had}(\text{nb})$	41.576±0.083	41.566±0.079	41.411±0.074	41.53±0.09
R_e	20.64±0.09	20.93±0.14	20.78±0.11	20.82±0.14
R_μ	20.88±0.07	20.70±0.09	20.84±0.10	20.79±0.07
R_τ	20.78±0.08	20.78±0.15	20.75±0.14	20.99±0.12
$A_{\rm FB}^{0,\,e}$	0.0187±0.0039	0.0179±0.0051	0.0148±0.0063	0.0104±0.0052
$A_{\rm FB}^{0,\,\mu}$	0.0179±0.0025	0.0153±0.0026	0.0176±0.0035	0.0146±0.0025
$A_{\rm FB}^{0,\,\tau}$	0.0196±0.0028	0.0223±0.0039	0.0233±0.0049	0.0178±0.0034

Table 1: Line shape and asymmetry parameters from to the data of the four LEP experiments.
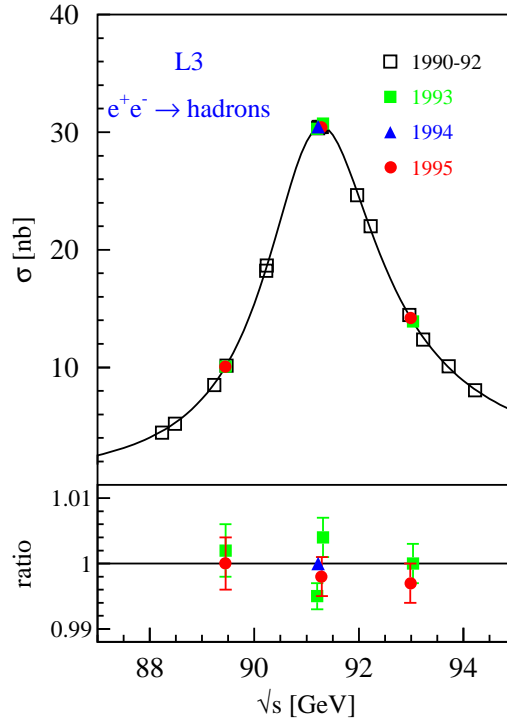

Figure 2: The hadronic line shape measured by the L3 collaboration.

2.4 Forward-backward lepton asymmetries

The forward backward asymmetry for a fermion f is defined as

$$A^f_{FB} = \frac{N_F - N_B}{N_F + N_B},$$

where N_F (N_B) is the number of events, where the fermion f is scattered in the incoming electron (positron) direction. On Born level the differential cross section w.r.t. the scattering angle is given by

$$\frac{\partial \sigma}{\partial \cos \theta} = \sigma_{tot} \left(\frac{3}{8}(1 + \cos^2 \theta) + A_{FB} \cos \theta \right),$$

which is only weakly modified by radiative corrections. For pure Z exchange the forward backward asymmetry can be expressed as

$$A^{0,f}_{FB} = \frac{3}{4} \mathcal{A}_e \mathcal{A}_f$$

with $\mathcal{A}_f = \frac{2 g_{Vf} g_{Af}}{g^2_{Vf} + g^2_{Af}}$.

g_{Vf}, (g_{Af}) denotes the vector (axial vector) coupling of the Z to the fermion f. The ratio of these two coupling is given by the weak mixing angle

$$\frac{g_{Vf}}{g_{Af}} = 1 - 4 Q_f \sin^2 \theta^f_{eff}.$$

Figure 3 shows the differential cross section $e^+ e^- \to \mu^+ \mu^-$ at the three energies obtained by DELPHI. The energy dependence of A_{FB} is given by the $\gamma - Z$ interference and contains little information on electroweak quantities. For that reason the experiments fit the asymmetries at the different energies, together with the lineshape, leaving only $A^{0,\ell}_{FB}$, $\ell = e, \mu, \tau$ as additional free parameters. The results are included in references [2–5] and table 1. The combined results are

$$\begin{aligned}
A^{0,e}_{FB} &= 0.0160 \pm 0.0024 \\
A^{0,\mu}_{FB} &= 0.0162 \pm 0.0013 \\
A^{0,\tau}_{FB} &= 0.0201 \pm 0.0018 \\
A^{0,\ell}_{FB} &= 0.0174 \pm 0.0010
\end{aligned}$$

2.5 τ Polarization

The mean τ polarization as a function of the scattering angle is given by:

$$\mathcal{P}_\tau(\cos \theta) = -\frac{\mathcal{A}_\tau (1 + \cos^2 \theta) + 2\mathcal{A}_e \cos \theta}{1 + \cos^2 \theta + 2\mathcal{A}_\tau \mathcal{A}_e \cos \theta}$$

From a measurement of the angular dependence of $\mathcal{P}_\tau$, $\mathcal{A}_e$ and $\mathcal{A}_\tau$ can thus be determined separately with almost no correlation.

The τ polarization can be extracted from the energy and decay angles of the τ decay products. This is illustrated for four different decay modes in figure 4.

Figure 5 shows the polarization as a function of the scattering angle from the L3 analysis.
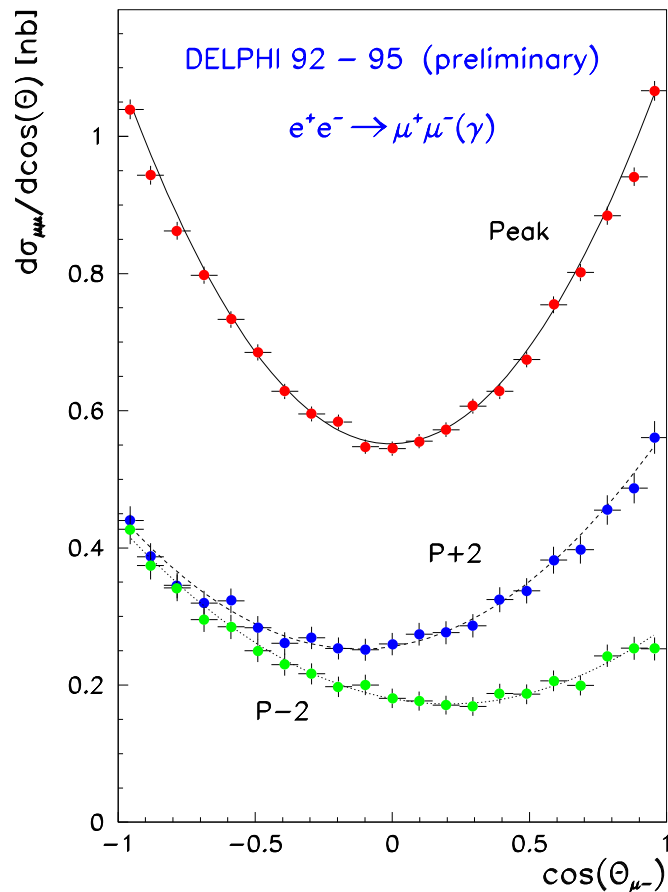
Figure 3: Differential cross section $e^+e^- \to \mu^+\mu^-$ measured by DELPHI.

The results of the different experiments are described in [6–9] and summarized in figure 6. Combining them yields

$$
\begin{aligned}
\mathcal{A}_e &= 0.1382 \pm 0.0076, \\
\mathcal{A}_\tau &= 0.1401 \pm 0.0067, \\
\mathcal{A}_\ell &= 0.1393 \pm 0.0050,
\end{aligned}
$$

where $\mathcal{A}_\ell$ denotes the result assuming lepton universality.

2.6 Z-lepton couplings

Since Γ_ℓ depends on the squared sum of the the vector and axial vector couplings $(g_{V\ell}^2 + g_{A\ell}^2)$ and the coupling parameter $\mathcal{A}_\ell$ that determines the asymmetries on the ratio $\left(\frac{g_{V\ell}}{g_{A\ell}}\right)$ the two couplings can be determined separately. Table 2 summarizes the result with and without the assumption of lepton universality. Also shown are the results if the left-right asymmetry measured at SLD [10] is included. The LEP results are shown in figure 7 together with the Standard Model prediction and the SLD result. The LEP data agree well with lepton universality. Also good agreement with the prediction and with the SLD result can be seen.
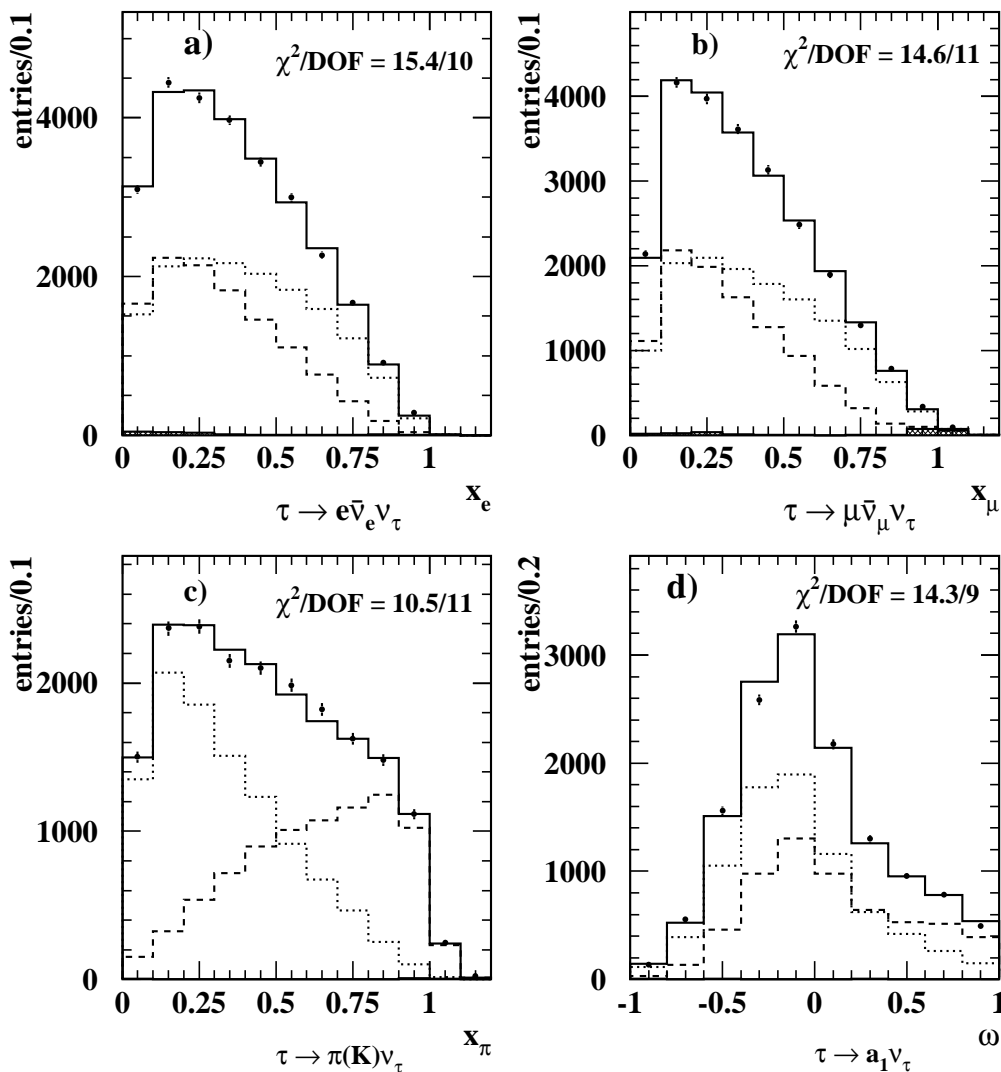
6

OPAL

Figure 4: Polarization sensitive variable for τ decays in the OPAL analysis for a) $\tau \to e \bar{\nu} \nu$, b) $\tau \to \mu \bar{\nu} \nu$, c) $\tau \to \pi \nu$ and d) $\tau \to a_1 \nu$. For a)-c) the sensitive variable plotted is the normalized energy of the charged decay-particle. For d) the variable is an optimized variable constructed from the a_1 energy and the decay angles in the a_1 decay. The points with the error bars represent the data, the dashed line the prediction for positive polarized taus and the dotted line for negative polarized tau. The solid line is a fit to the data with the polarization left free.
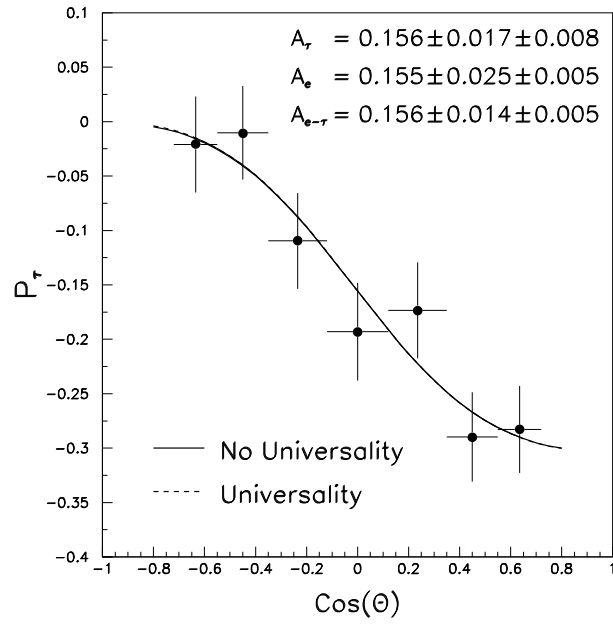
Figure 5: τ polarization as a function of the scattering angle from the L3 collaboration. The line represent a fit to the data with (dashed) and without (solid) the assumption of lepton universality.
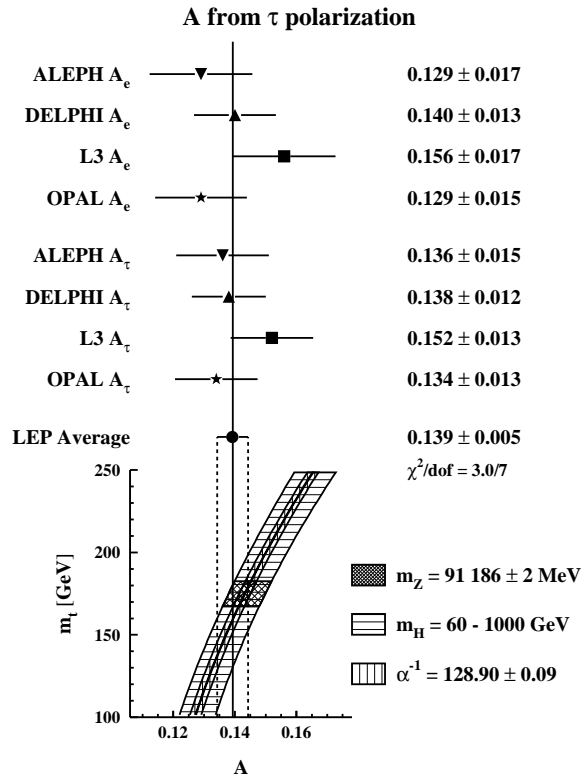

Figure 6: Measurement of the τ polarization and its asymmetry at LEP.

| | Without Lepton Universality: | |
	LEP	LEP+SLD
g_{Ve}	-0.0368 ± 0.0015	-0.03828 ± 0.00079
$g_{V\mu}$	-0.0372 ± 0.0034	-0.0358 ± 0.0030
$g_{V\tau}$	-0.0369 ± 0.0016	-0.0367 ± 0.0016
g_{Ae}	-0.50130 ± 0.00046	-0.50119 ± 0.00045
$g_{A\mu}$	-0.50076 ± 0.00069	-0.50086 ± 0.00068
$g_{A\tau}$	-0.50116 ± 0.00079	-0.50117 ± 0.00079
	With Lepton Universality:	
	LEP	LEP+SLD
$g_{V\ell}$	-0.03688 ± 0.00085	-0.03776 ± 0.00062
$g_{A\ell}$	-0.50115 ± 0.00034	-0.50108 ± 0.00034

Table 2: Results for the effective vector and axial-vector couplings derived from the combined LEP data without and with the assumption of lepton universality. For the right column the SLD measurement of A_{LR} is also included.
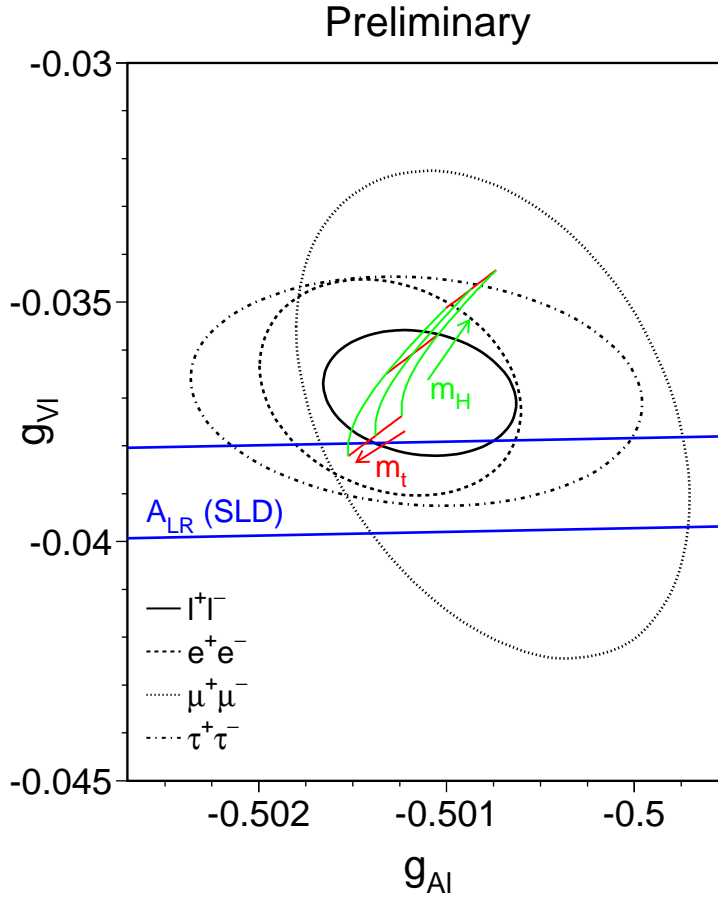

Figure 7: Contours of 68% probability in the $g_{V\ell}$-$g_{A\ell}$ plane from LEP measurements. The solid contour results from a fit assuming lepton universality. Also shown is the one standard deviation band resulting from the A_{LR} measurement of SLD. The grid corresponds to the Standard Model prediction for $m_{\mathrm{t}} = 175 \pm 6\,\mathrm{GeV}$ and $m_{\mathrm{H}} = 300^{+700}_{-240}\,\mathrm{GeV}$. The arrows point in the direction of increasing values of m_{t} and m_{H}.

9

3 Electroweak Physics with Quarks

b- and c-quarks can be tagged with high efficiency and purity, so that they can be used for electroweak analyses. Two types of quantities are of basic interest:

- the forward-backward asymmetries $A_{\mathrm{FB}}^{\mathrm{b}}$, $A_{\mathrm{FB}}^{\mathrm{c}}$,
- the normalized partial widths R_{b}^{0}, R_{c}^{0} ($R_{q}^{0} = \frac{\Gamma_{q}}{\Gamma_{\mathrm{had}}}$)[1].

As can be seen from table 3 the quark asymmetries are an efficient measure of $\sin^2 \theta_{eff}^l$. The sensitivity is about a factor three larger than for charged leptons and the total statistics for b and c quarks is each about equal to the sum of all lepton species. In principle the forward-backward asymmetries depend on the product of the initial and final state coupling. However if $\sin^2 \theta_{eff}^q$ is written as $\sin^2 \theta_{eff}^q = \sin^2 \theta_{eff}^l + \delta_q$, in the Standard Model δ_c is constant. The variation of δ_b is about the same size as for $\sin^2 \theta_{eff}^l$, but the sensitivity of $A_{\mathrm{FB}}^{\mathrm{b}}$ to δ_b is two orders of magnitude smaller than the sensitivity to $\sin^2 \theta_{eff}^l$.

	$\frac{\partial A_{FB}}{\partial \sin^2 \theta}$	$\frac{\Gamma_f}{\Gamma_Z}$
e, μ, τ	1.7	$3 \times 3.4\%$
c	4.3	12%
b	5.6	15%

Table 3: Sensitivity of A_{FB} to $\sin^2 \theta_{eff}^l$ and Z branching ratio for charged leptons, c- and b-quarks.

Contrary in R_{b}^{0}, R_{c}^{0} practically all QED, QCD and electroweak propagator corrections cancel and only corrections to the $Z \to q\bar{q}$ vertex remain. R_{c}^{0} is thus predicted by the Standard Model with a very small error. In this model R_{b}^{0} depends only on the top quark mass, however in supersymmetric extensions also some dependence on the stop and chargino sector arises.

3.1 Tagging methods

Basically three methods exist to tag b- and c-quarks:

- lifetime tags, using impact parameters or secondary vertices for b-quarks,
- high momentum leptons in jets for b- and c-quarks,
- exclusively or inclusively reconstructed D mesons, mainly for c-quarks.

3.1.1 Lifetime tags

The lifetime tags provide the purest and most efficient methods to tag b-quarks. Basically two principle methods exist. Either the experiments try to reconstruct secondary vertices and measure the distance of such vertices to the primary one or the beam-spot (DELPHI, OPAL) or the presence of tracks with a large impact parameter with respect to the primary vertex is used as tagging method (ALEPH, DELPHI, L3). For the tagging of b-hemispheres both methods give purities of more than 90% for efficiencies of more than 20%. Recently ALEPH combined the lifetime tag with a cut on invariant masses and obtained a 98% purity at an efficiency of 23% [11]. Figure 8 shows the uds- and c-efficiency for this tag as a function of the b-tagging efficiency.

---

[1] The ^{0} always indicates that a quantity is corrected to pure Z exchange.
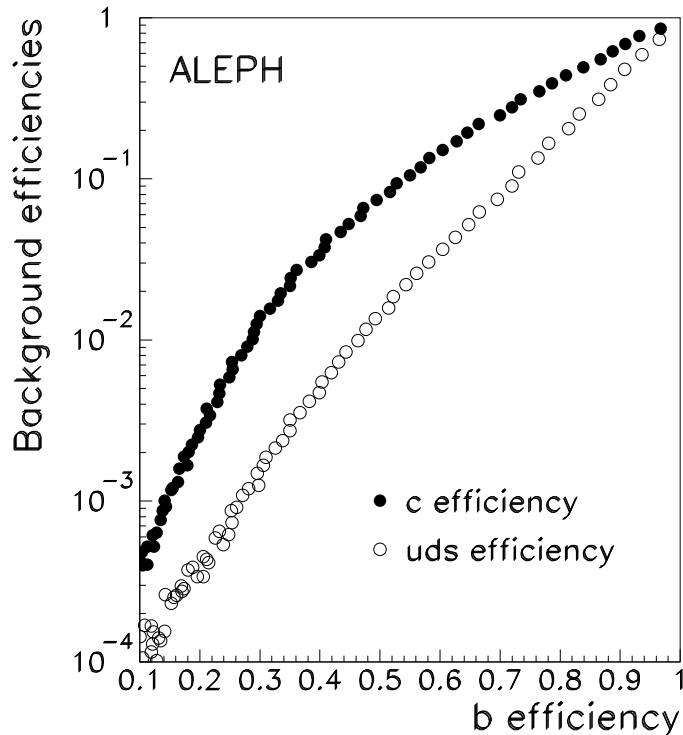
Figure 8: uds- and c-efficiency as a function of the b-efficiency for the ALEPH lifetime plus mass tag.

3.1.2 Lepton tags

High momentum leptons in jets are used since long to tag b and c quarks. An almost pure sample from prompt $b \to \ell$ decays can be obtained by cutting on the transverse momentum of the lepton relative to the jet axis. On the contrary a clean separation of leptons from charm and those from b-cascade leptons and misidentified hadrons is not possible.

OPAL improved recently their lepton tagging by the use of additional variables measured from the jet to which the lepton is associated [21]. As can be seen from figure 9 this give a very good purity for $b \to \ell$ and also a reasonable purity for $c \to \ell$.

Although efficiency and purity for the lepton tag are not as good as for the lifetime tags the lepton measurements still provide the most accurate results on the b-asymmetry, since the lepton charge is an efficient indicator of the quark charge.

3.1.3 D-meson tags

D mesons indicate the presence of either c or b quarks. However the D's from charm tend to have a higher momentum than the ones from B-decays. Further separation of the two quark flavours, more independent on the knowledge of fragmentation properties, is possible using lifetime tags as described above.

Three different methods to tag D-mesons are used:
  − exclusive $D^{*\pm}$ reconstruction: First a $D^{0 \, 2)}$ is reconstructed and then the D^0 is com-

---

2) If not mentioned explicitly, charge conjugate modes are always included.
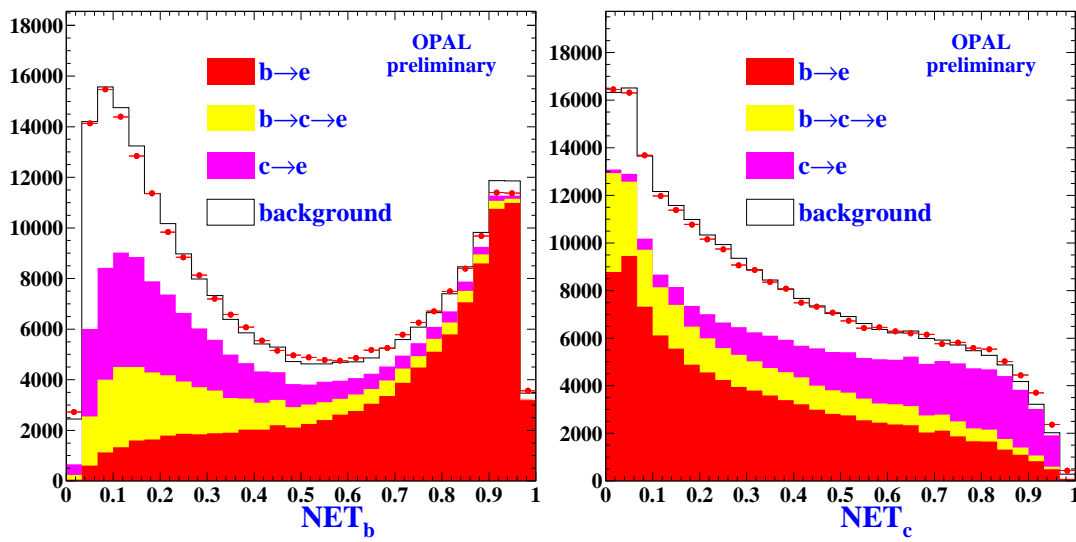
Figure 9: Network output for the different electron sources in the OPAL lepton tag.

bined with a π^+ to a D^{*+}. Due to the small $D^{*+} - D^0$ mass difference the available phase space for the π^+ is very small leading to a good resolution in the mass difference. For this reason many D^0 decay modes can be used, even some where the D^0 is reconstructed only partially, still giving a small combinatorial background.

– inclusive $D^{*\pm}$ reconstruction: Due to the small $D^{*+} - D^0$ mass difference the π^+ from the D^{*+} decay is forced to follow the D^{*+} flight direction and to have a relatively low momentum. This leads to a small transverse momentum of the decay pion with respect to the jet axis. Due to the large background an event by event tag is not possible with this method. However the number of D^{*+}-mesons in a sample can be obtained from the access of particles at low p_t in the p_t distribution.

– exclusive charmed hadron reconstruction: Clean signals can be obtained for basically all weakly decaying charmed hadrons. However the combinatorial background is rather high for all of these channels.

3.2 Combination of data

The combination of the LEP heavy flavour data is more complicated than for the lineshape and τ polarization measurements. In some cases more than one quantity is measured in the same analysis leading to statistical correlations and in all cases assumptions on heavy flavour production and decay properties are needed leading to correlations in the systematic errors between different measurements. In addition some measurements depend explicitly on the values assumed for the other quantities, e.g. the double tag measurements of R_b depend on the value assumed for R_c. All this makes it necessary to have a well defined procedure to combine the electroweak results with heavy flavours.

In addition SLD produces measurements on R_b that are comparable to the ones at LEP and measurements of the polarized forward-backward asymmetries of b- and c-quarks that are physically independent of the LEP observables, but need the same assumptions and are therefore systematically correlated with the LEP numbers.

The LEP experiments and SLD have agreed on a common set of input parameters and their errors to be used for the heavy flavour analyses and a procedure to combine the results. A detailed write-up of the full procedure can be found in [13]. The input

parameters have been updated recently [14] to take into account new measurements. The main updates are:

- All numbers taken from PDG have been updated with the 96 edition [15].
- Acceptance biases to the QCD corrections to the forward backward asymmetries have been evaluated. The experimental cuts select predominantly high momentum quarks. On the contrary the QCD correction, which has a total size of about 3% of the asymmetry, is mainly due to low momentum quarks with a random direction after hard gluon radiation. The QCD correction is thus reduced by about a factor of two.
- The production rates of charmed hadrons are taken from LEP measurements. These rates enter directly in the interpretation of charmed hadron cross sections in terms of R_c and at second order in the estimate of the charm-background in the R_b analyses. Up to now these rates have been evaluated from data taken at lower energy. This needed however the assumption that the fragmentation process is energy independent.
- The probability that a gluon splits into a $c\bar{c}$ pair is measured by OPAL [16]. This number is used in all the LEP/SLD analyses now. The ratio $\frac{g \to b\bar{b}}{g \to c\bar{c}}$ is still taken from theory but DELPHI has presented a preliminary measurement of the gluon splitting to $b\bar{b}$ which is consistent with the used number [17].

3.3 Quark asymmetries

For $A_{\mathrm{FB}}^{\mathrm{b}}$ there are two methods with about equal precision:

- lepton tags,
- lifetime tags combined with a jet charge technique.

The lepton tag analyses measure $A_{\mathrm{FB}}^{\mathrm{b}}$ either in a sample of high p and p_t leptons or as a function of the lepton momentum and transverse momentum. In both cases the Monte Carlo is used to predict the sample composition that is needed to correct the raw asymmetry. In addition the data have to be corrected for QCD- effects and $b\bar{b}$ mixing. However all corrections are well under control and the measurements are statistically limited. Most of the needed input parameters like the average mixing and semileptonic branching ratios are measured by the LEP experiments themselves sometimes even in the same analyses. The results of the experiments on $A_{\mathrm{FB}}^{\mathrm{b}}$ with leptons and the lepton fits can be found in [18–21].

For the lifetime plus jetcharge measurements first a $b\bar{b}$ sample is selected with a lifetime tag and the quark charge is measured from the mean jet charge on a statistical basis. Using the sum and the difference of the two hemisphere jet charges the charge tagging efficiency is extracted simultaneously from data. Only corrections due to hemisphere correlations and light quark backgrounds need to be taken from Monte Carlo. Effects from b-mixing and QCD are already included in the measured charge tagging efficiency. The results of the four experiments are reported in [22, 19, 23].

Figure 10 a) summarizes the results obtained with the two methods. In addition DELPHI and OPAL report results on $A_{\mathrm{FB}}^{\mathrm{b}}$ with D mesons. However this is basically to take care of the correlation with $A_{\mathrm{FB}}^{\mathrm{c}}$ and the results are not competitive with the analyses presented here.

$A_{\mathrm{FB}}^{\mathrm{c}}$ is either measured with leptons together with $A_{\mathrm{FB}}^{\mathrm{b}}$ or using D-mesons. The results of the D-meson analyses can be found in [24, 19, 25]. Figure 10 b) summarizes the experimental results.
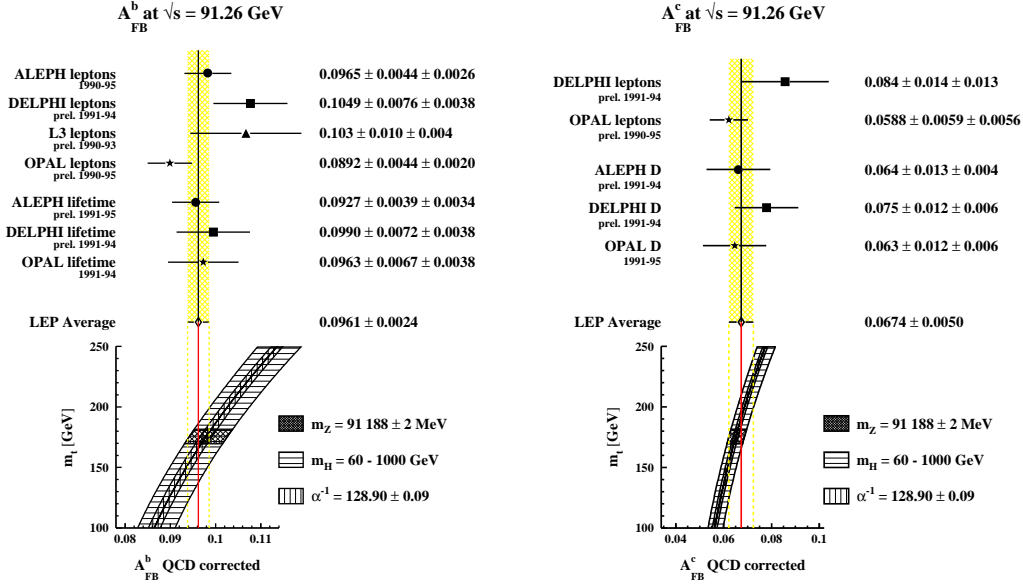
A^b_{FB} at $\sqrt{s} = 91.26$ GeV

ALEPH leptons 1990-95	$0.0965 \pm 0.0044 \pm 0.0026$
DELPHI leptons prel. 1991-94	$0.1049 \pm 0.0076 \pm 0.0038$
L3 leptons prel. 1990-93	$0.103 \pm 0.010 \pm 0.004$
OPAL leptons prel. 1990-95	$0.0892 \pm 0.0044 \pm 0.0020$
ALEPH lifetime prel. 1991-95	$0.0927 \pm 0.0039 \pm 0.0034$
DELPHI lifetime prel. 1991-94	$0.0990 \pm 0.0072 \pm 0.0038$
OPAL lifetime 1991-94	$0.0963 \pm 0.0067 \pm 0.0038$
LEP Average	0.0961 ± 0.0024

$m_Z = 91\ 188 \pm 2$ MeV
$m_H = 60$ - 1000 GeV
$\alpha^{-1} = 128.90 \pm 0.09$

m_t [GeV], A^b_{FB} QCD corrected

A^c_{FB} at $\sqrt{s} = 91.26$ GeV

DELPHI leptons prel. 1991-94	$0.084 \pm 0.014 \pm 0.013$
OPAL leptons prel. 1990-95	$0.0588 \pm 0.0059 \pm 0.0056$
ALEPH D prel. 1991-94	$0.064 \pm 0.013 \pm 0.004$
DELPHI D prel. 1991-94	$0.075 \pm 0.012 \pm 0.006$
OPAL D 1991-95	$0.063 \pm 0.012 \pm 0.006$
LEP Average	0.0674 ± 0.0050

$m_Z = 91\ 188 \pm 2$ MeV
$m_H = 60$ - 1000 GeV
$\alpha^{-1} = 128.90 \pm 0.09$

m_t [GeV], A^c_{FB} QCD corrected

Figure 10: a) A^b_{FB} and b) A^c_{FB} from the LEP experiments compared to the Standard Model prediction.

3.4 R_c

R_c is measured with several methods:

- leptons(ALEPH, DELPHI): $R_c \cdot BR(c \to \ell)$ can be obtained from leptons at low p_t. This measurement is systematically limited by $BR(c \to \ell)$ which has to be inferred from low energy data.

- single/double tag (ALEPH, DELPHI): In a single/double tag measurement R_c can be extracted without knowing the tagging efficiency. Only Monte Carlo corrections for background and hemisphere correlations are needed. ALEPH and DELPHI have presented such measurements for R_c. ALEPH uses reconstructed D-mesons, which suffer from the low tagging efficiency. DELPHI uses instead a low p_t pion $D^{*\pm}$ tag. This measurement is however limited by the understanding of the background systematics in the single tag sample.

- inclusive/exclusive double tag (ALEPH, DELPHI, OPAL): This method tries to overcome the two problems in the single/double tag measurements described above. In a first step $R_c \cdot P(c \to D^{*+} \to \pi^+ D^0)$ is measured from exclusively reconstructed $D^{*\pm}$, where $P(c \to D^{*+} \to \pi^+ D^0)$ is the probability that a c-quark fragments into a D^{*+} which subsequently decays in $D^0 \pi^+$. In a second step $P(c \to D^{*+} \to \pi^+ D^0)$ is measured from the low p_t pion rate opposite to an exclusively reconstructed $D^{*\pm}$. The disadvantage of this method is that the D^0 reconstruction efficiency in the single tag sample needs to be known from simulation.

- charm counting (DELPHI, OPAL): The production rate of a single charmed hadron D is proportional to $R_c \cdot f(D)$ where $f(D)$ is the probability that a charm quark fragments into a hadron D. Since all c-quarks end up in a weakly decaying particle

14

the rates of those hadrons have to add up to one:

$$f(D^0) + f(D^+) + f(D_s) + 1.15f(\Lambda_c) = 1$$

where the factor 1.15 accounts for up to now unmeasured charmed strange baryons. If the reconstruction efficiencies are known R_c can therefore be measured from the sum of four single tag measurements.

The results of the different measurements are presented in [26–28] and summarized in figure 11.
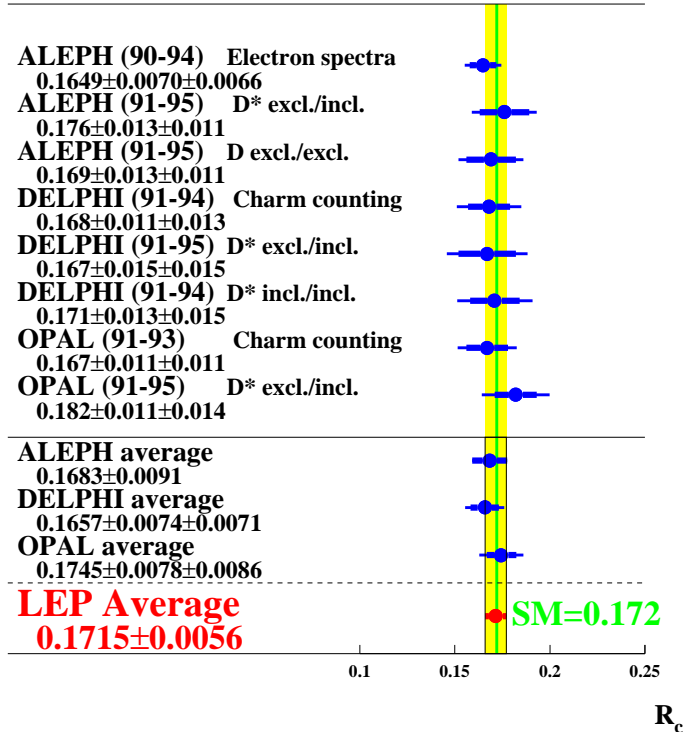

Figure 11: The measurements of R_c at LEP.

3.5 R_b

All precise measurements of R_b are single/double tag measurements using a lifetime tag. In a recent analysis ALEPH has upgraded this method by using five different tags [11]:

1) a very pure impact parameter plus mass cut b-tag,
2) a neural net event shape b-tag,
3) a high p_t lepton b-tag,
4) a neural net c-tag,
5) an impact parameter uds-tag.

All five single and 15 double tag rates are measured in their analysis. If all hemisphere correlations and the background efficiencies for the tag 1) are taken from Monte Carlo, R_b and all other efficiencies can be measured from data. The inclusion of the additional tags does not alter the systematic uncertainty, but gives a substantial reduction in the statistical error.

All experiments include their data up to 1994 now, so that most of the LEP 1 statistics is used. However some substantial improvements in the methods can still be

expected. Figure 12 summarizes the results which are presented in [11, 29–31]. Also the result from SLD [10] is shown and included in the mean.
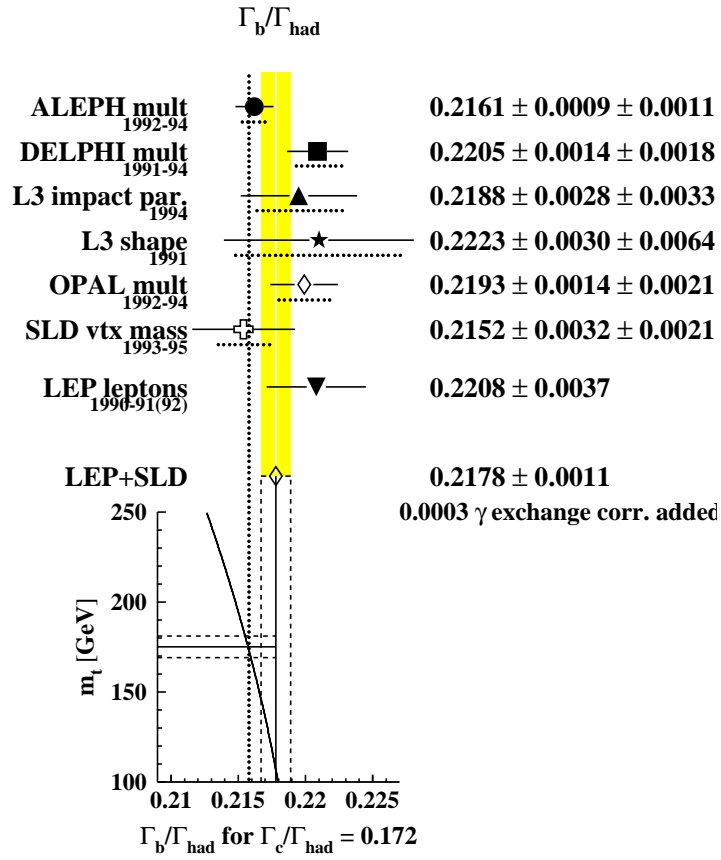

Figure 12: The measurements of R_{b} at LEP and SLD.

3.6   Results

All measurements presented here and the polarized forward backward asymmetries from SLD [10] have been combined with the method described in section 3.2. The following results have been obtained:

$$
\begin{aligned}
R_{\mathrm{b}}^0 &= 0.2178 \pm 0.0011 \\
R_{\mathrm{c}}^0 &= 0.1715 \pm 0.0056 \\
A_{\mathrm{FB}}^{0,\mathrm{b}} &= 0.0979 \pm 0.0023 \\
A_{\mathrm{FB}}^{0,\mathrm{c}} &= 0.0735 \pm 0.0048 \\
\mathcal{A}_{\mathrm{b}} &= 0.863 \pm 0.049 \\
\mathcal{A}_{\mathrm{c}} &= 0.625 \pm 0.084
\end{aligned}
$$

The correlation matrix can be found in table 4. The dominant error sources for the four LEP quantities are listed in table 5. The errors on $\mathcal{A}_{\mathrm{b}}$ and $\mathcal{A}_{\mathrm{c}}$ are completely dominated by statistics and detector dependent systematics.

16

	R_{b}^0	R_{c}^0	$A_{\mathrm{FB}}^{0,\,\mathrm{b}}$	$A_{\mathrm{FB}}^{0,\,\mathrm{c}}$	$\mathcal{A}_{\mathrm{b}}$	$\mathcal{A}_{\mathrm{c}}$
R_{b}^0	1.00	−0.23	0.00	0.00	−0.03	0.01
R_{c}^0	−0.23	1.00	0.04	−0.06	0.05	−0.07
$A_{\mathrm{FB}}^{0,\,\mathrm{b}}$	0.00	0.04	1.00	0.10	0.04	0.02
$A_{\mathrm{FB}}^{0,\,\mathrm{c}}$	0.00	−0.06	0.10	1.00	0.01	0.10
$\mathcal{A}_{\mathrm{b}}$	−0.03	0.05	0.04	0.01	1.00	0.12
$\mathcal{A}_{\mathrm{c}}$	0.01	−0.07	0.02	0.10	0.12	1.00

Table 4: The correlation matrix for the electroweak parameters from the heavy-flavour fit

source	R_{b} $\cdot 10^{-3}$	R_{c} $\cdot 10^{-3}$	A_{FB}^{b} $\cdot 10^{-3}$	A_{FB}^{c} $\cdot 10^{-3}$
statistics	0.67	3.7	2.0	4.1
internal syst.	0.53	2.9	0.8	2.2
QCD effects	0.31	0.4	0.3	0.4
$BR(D \to K^0 X)$	0.22	0.3	0	0
D decay mult.	0.29	0.5	0	0
$BR(D^0 \to K^- \pi^+)$	0.03	0.2	0	0
$BR(D^+ \to K^- \pi^+ \pi^+)$	0.10	0.3	0	0
$BR(D_s \to \phi \pi^+)$	0.06	1.1	0	0
Br(c $\to \ell$)	0.03	2.2	0.2	0.3
gluon splitting	0.44	0.8	0	0
b fragmentation	0.15	0.1	0.2	0.1
light quarks	0.17	0.3	0.4	0
total	1.12	5.6	2.3	4.8

Table 5: Dominant error sources of the electroweak parameters. For R_{b} the errors are given with R_{c} fixed to 0.172.

4 Interpretation of Electroweak Data

4.1 The weak mixing angle

All asymmetries measured at LEP and SLD can be interpreted in terms of the effective weak mixing angle $\sin^2 \theta_{eff}^l$. If new physics appears only via radiative corrections this is true also for the quark asymmetries, as explained in section 3. The results for $\sin^2 \theta_{eff}^l$ from the different observables are summarized in figure 13. Their average, using all LEP and SLD results, is

$$\sin^2 \theta_{eff}^l = 0.23165 \pm 0.00024.$$

The total χ^2 for the average is 12.8 for 6 degrees of freedom which corresponds to a probability of about 5%. Responsible for the large χ^2 are about equally the left-right asymmetry from SLD and A_{FB}^b from LEP.
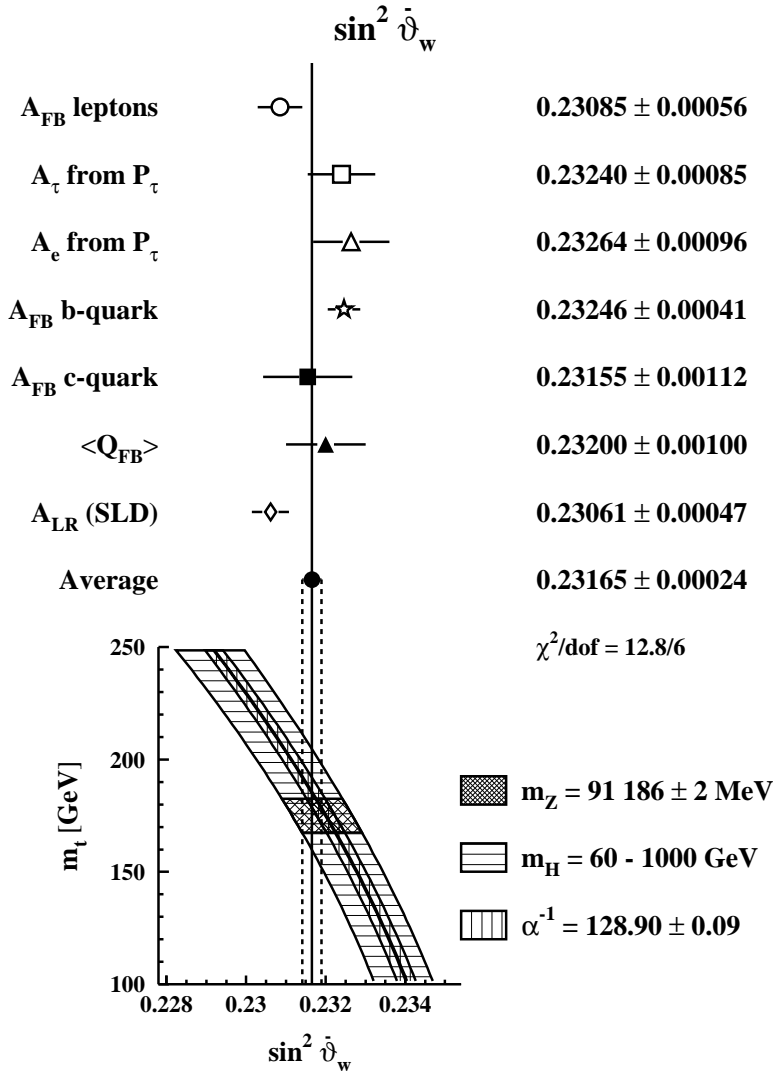
Figure 13: The measurements of $\sin^2 \theta_{eff}^l$ at LEP and SLD.

In any interpretation of $\sin^2 \theta_{eff}^l$ there is an additional uncertainty of 0.00023 coming from the uncertainty in the hadronic vacuum polarization in the running of the electromag-

18

netic coupling constant $\Delta\alpha$. This uncertainty can be only reduced by better measurements of the total hadronic cross section at lower energies.

4.2   Quark couplings

The polarized forward backward asymmetries from SLD measure directly the coupling parameter for b- and c-quarks $\mathcal{A}_b$, $\mathcal{A}_c$. At LEP these parameters can be obtained from the ratio of the quark asymmetries and $\mathcal{A}_\ell$ from the lepton asymmetries. Table 6 summarizes the quark coupling parameters for the LEP and LEP+SLD data and their Standard Model prediction. For the LEP only data the LEP value $\mathcal{A}_\ell = 0.1466 \pm 0.0033$ has been used. For the LEP+SLD the combined value $\mathcal{A}_\ell = 0.1500 \pm 0.0025$ was used instead.

	LEP	LEP+SLD	Standard Model
$\mathcal{A}_b$	0.890 ± 0.029	0.867 ± 0.022	0.935
$\mathcal{A}_c$	0.667 ± 0.047	0.646 ± 0.040	0.667

Table 6: LEP and LEP+SLD results on $\mathcal{A}_b$ and $\mathcal{A}_c$ compared to the Standard Model. Within the given precision the prediction is without uncertainty.

The bad agreement of $\mathcal{A}_b$ with the prediction is another manifestation of the differences in the $\sin^2 \theta^l_{eff}$ results.

4.3   Standard Model fits

If new physics appears only via radiative corrections basically all electroweak observables can be expressed in terms of three quantities: Γ_ℓ, $\sin^2 \theta^l_{eff}$ and m_W. Figure 14 shows the bands obtained from the world averages of these three quantities in the $\varepsilon_1 - \varepsilon_3$-plane defined by G. Altarelli et al. [32]. The three bands cross each other in the region predicted by the Standard Model. This suggests that the data are globally consistent with this model.

Since the data agree well with the predictions of the Standard Model they can be used to constrain its unknown parameters via their effects on the radiative corrections. To constrain the Higgs sector from the electroweak precision data a global fit to all data has been performed. For the fit the program ZFITTER [33] has been used, however it has been shown that different programs give identical results [34, 35].

For all parameters apart from R_b, which depends only on m_t, the effects induced by the top and the Higgs particle are strongly correlated. The information on the Higgs boson mass is therefore improved significantly, if the direct measurement of m_t from the Tevatron [36] is imposed in the fit. Apart from the LEP and SLD data also m_W from the Tevatron [37] and $\sin^2 \theta = 1 - m_W^2/m_Z^2$ from ν-nucleon scattering [38–40] are used. The results of the fit are:

$$\log(m_H) = 2.17^{+0.30}_{-0.35}$$
$$\alpha_s(m_Z^2) = 0.120 \pm 0.003$$

The value of the strong coupling constant agrees well with the world average of 0.118 ± 0.003 [15] which was obtained without the observables used here. The χ^2 of the fit is 19 for 14 degrees of freedom which corresponds to a probability of 16%. From this it can be concluded that the data agree globally well with each other and with the Standard Model.

19

		Measurement with Total Error	Standard Model	Pull
a)	LEP			
	line-shape and lepton asymmetries:			
	m_Z [GeV]	91.1863 ± 0.0020	91.1861	0.1
	Γ_z [GeV]	2.4946 ± 0.0027	2.4960	-0.5
	σ_0^{had} [nb]	41.508 ± 0.056	41.465	0.8
	R_ℓ	20.778 ± 0.029	20.757	0.7
	$A_{\mathrm{FB}}^{0,\ell}$	0.0174 ± 0.0010	0.0159	1.4
	+ correlation matrix			
	τ polarization:			
	$\mathcal{A}_\tau$	0.1401 ± 0.0067	0.1458	-0.9
	$\mathcal{A}_e$	0.1382 ± 0.0076	0.1458	-1.0
	b and c quark results:			
	R_{b}^0	0.2179 ± 0.0012	0.2158	1.8
	R_{c}^0	0.1715 ± 0.0056	0.1723	-0.1
	$A_{\mathrm{FB}}^{0,\mathrm{b}}$	0.0979 ± 0.0023	0.1022	-1.8
	$A_{\mathrm{FB}}^{0,\mathrm{c}}$	0.0733 ± 0.0049	0.0730	0.1
	+ correlation matrix			
	$q\bar{q}$ charge asymmetry:			
	$\sin^2 \theta_{eff}^l \; (< Q_{FB} >)$	0.2320 ± 0.0010	0.23167	0.3
b)	SLD			
	$\sin^2 \theta_{eff}^l \; (A_{LR})$	0.23061 ± 0.00047	0.23167	-2.2
	R_{b}^0	0.2149 ± 0.0038	0.2158	-0.2
	$\mathcal{A}_{\mathrm{b}}$	0.863 ± 0.049	0.935	-1.4
	$\mathcal{A}_{\mathrm{c}}$	0.625 ± 0.084	0.667	-0.5
c)	$p\bar{p}$ and νN			
	m_W [GeV] ($p\bar{p}$)	80.356 ± 0.125	80.353	0.3
	$1 - m_W^2/m_Z^2$ (νN)	0.2244 ± 0.0042	0.2235	0.2
	m_t [GeV] ($p\bar{p}$)	175 ± 6	172	0.5

Table 7: The quantities used in the electroweak fit. The second column shows the experimental results, the third column the Standard Model prediction after the fit and the fourth column the difference, normalized to the experimental error.

20

All data used are summarized in table 7 together with the Standard Model predictions. The deviations from the prediction follow perfectly the expectation.

Figure 15 shows the variation of the fit-χ^2 with the Higgs mass. The shaded band gives an estimate of the theoretical uncertainty. Including the theoretical error an upper limit of $m_H < 550\,\mathrm{GeV}$ can be derived at 95% confidence level.

5 Measurement of V_{cb} at LEP

The differential decay rate of the decay $\bar{B}^0 \to D^{*+}\ell\bar{\nu}_\ell$ with respect to the velocity of the D^{*+} in the B rest frame can be written as

$$\frac{\partial\Gamma}{\partial\omega} = \frac{G_F^2}{48\pi^2}m_{D^{*+}}^3(m_{B^0} - m_{D^{*+}})^2 k(\omega)\sqrt{\omega^2 - 1} \times \mathcal{F}^2(\omega)|V_{cb}|^2,$$

where $k(\omega)$ is a known kinematic function. For the form factor $\mathcal{F}(\omega)$, HQET predicts [41]:

$$\begin{aligned}
\mathcal{F}(\omega) &= \mathcal{F}(1)[1 - \rho^2(1 - \omega) + c(1 - \omega)^2] \\
\mathcal{F}(1) &= 0.91 \pm 0.04
\end{aligned}$$

where ρ^2 and c are in principle free parameters, however the correlation between the two is also known from HQET with good precision [41].

The same analysis can also be performed at machines running at the $\Upsilon(4S)$, however in a very complementary way:

- the data sample is typically larger at the $\Upsilon(4S)$-machines;
- at the $\Upsilon(4S)$ the B's are at rest, at LEP the B-momentum needs to be reconstructed;
- at the $\Upsilon(4S)$ the momentum of the pion in the $D^{*+} \to \pi^+D^0$ decay is very low and its acceptance very small close to the interesting limit $\omega \to 1$, at LEP however the π^+ momentum distribution is more or less independent of ω.

ALEPH, DELPHI and OPAL have performed analyses of V_{cb} using this decay [42–44]. $D^{*+}\ell$ events are selected in different D^0 decay channels with a typical efficiency of about 10% and a purity of about 80% independent of ω.

For the reconstruction of ω, the momentum vectors of the B and the D^{*+} need to be known. Since the D^{*+} is fully reconstructed, its momentum is measured with good precision. The $\bar{B}^0$ direction is reconstructed from the primary and secondary vertex positions. The energy is estimated from the D^{*+} and ℓ energies and from the missing momentum in the hemisphere of the $\bar{B}^0$. With this a resolution of $\Delta\omega < 0.1$ is obtained.

The data are then fitted with two free parameters, $\mathcal{F}(1)|V_{cb}|$ and ρ^2. Figure 16 a) shows the ALEPH data together with the fit prediction. Figure 16 b) shows the same data and prediction after correction for detector effects and the kinematic terms. Good agreement with the linear dependence predicted by HQET can be observed.

The LEP results on V_{cb} and ρ^2 are summarized in figure 17. One obtains [45]

$$\begin{aligned}
\mathcal{F}(1)|V_{cb}| &= (34.4 \pm 2.2)10^{-3}, \\
\rho^2 &= 0.56 \pm 0.13.
\end{aligned}$$

Applying a scale factor of 1.23 on the error to account for some disagreement between the different experiment yields for the world average [46]:

$$\begin{aligned}
\mathcal{F}(1)|V_{cb}| &= 0.0357 \pm 0.0021(\text{exp.}) \pm 0.0014(\text{curv.}), \\
\Longrightarrow \quad |V_{cb}| &= 0.0392 \pm 0.0027(\text{exp.}) \pm 0.0013.(\text{th.})
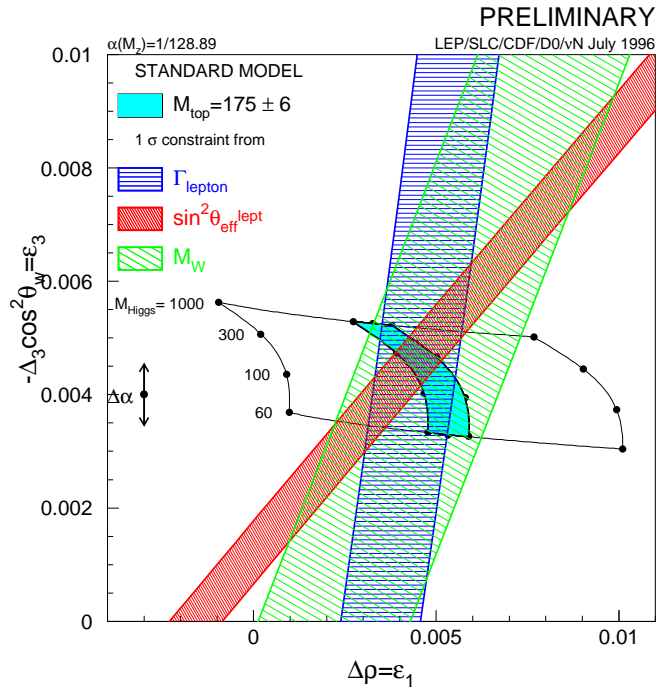\end{aligned}$$

21

Figure 14: Experimentally measured bands in the $\varepsilon_1 - \varepsilon_3$-plane from m_W, Γ_ℓ and $\sin^2 \theta_{eff}^l$ compared to the Standard Model prediction.
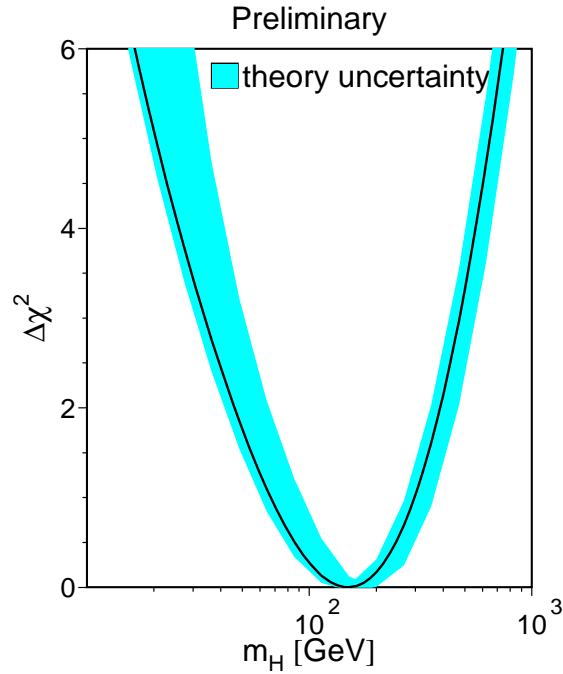

Figure 15: $\Delta\chi^2$ as a function of the Higgs mass. The shaded band gives an estimate of the theoretical uncertainty.

The result is in good agreement with the one obtained from the inclusive semileptonic decay rate $\mathrm{Br}(b \to c\ell\nu)$ at LEP:

$$|V_{cb}| = 0.0420 \pm 0.0005(\text{exp.}) \pm 0.0041(\text{th.}),$$

but with much smaller theoretical uncertainty.

6 $B\bar{B}$-mixing

B^0 and B_s^0 mesons mix with their antiparticles via box-diagrams, mainly involving top quark loops. The probability that a meson, which is produced at the time $t = 0$ as a particle B, decays at time t as its antiparticle $\bar{B}$ is given by

$$P(B \to \bar{B})(t) = \frac{\Gamma}{2} e^{-\Gamma t} (1 - \cos(\Delta m t)),$$

where Γ is the total B decay width and Δm the mass difference between the two CP-eigenstates. Δm depends on the elements of the CKM matrix:

$$
\begin{aligned}
\Delta m_{B^0} &\propto f_{B^0} |V_{td} V_{tb}^*|^2 \\
\Delta m_{B_s^0} &\propto f_{B_s^0} |V_{ts} V_{tb}^*|^2 \\
\frac{\Delta m_{B_s^0}}{\Delta m_{B^0}} &\propto \frac{f_{B_s^0}}{f_{B^0}} \left| \frac{V_{ts}}{V_{td}} \right|^2
\end{aligned}
$$

The form factors f_{B^0}, $f_{B_s^0}$ need to be calculated from QCD. Some of the uncertainties in the calculation drop out in the ratio.

At LEP, B-Mesons fly several millimetres with an approximate vertex resolution of about 300μm. The mixing probability can thus be observed as a function of the B-lifetime. To measure B-oscillations one needs need to
- identify the b-charge at production time,
- identify the b-charge at decay time,
- measure the proper time from production to decay.

6.1 B^0-oscillations

For the measurement of B^0-oscillations, a special B^0-tagging is not needed, since B_s^0-mesons oscillate much faster and all other b-hadrons don't oscillate. It is thus sufficient to reject background from light quark events.

6.1.1 Determination of the production charge

Generally the b-charge at production time is tagged by measuring the b-charge in the opposite hemisphere. Two methods are used:
- a high p_t lepton,
- a jetcharge algorithm combined with a lifetime b-tag.

Both methods provide a b-purity of $\approx 90\%$ and a charge mistag rate of $\approx 25\%$.

6.1.2 Determination of the decay charge

Again two methods are commonly used:
- a high p_t lepton,
- a $D^{*\pm}$-meson reconstructed either inclusively or exclusively.
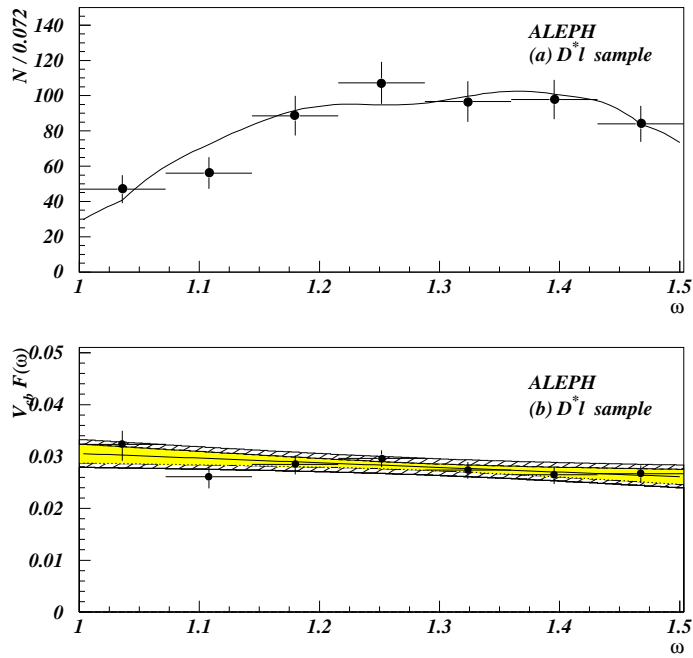
Figure 16: a) Differential event rate $dN/d\omega$ after cuts and background subtraction. The points are the data and the solid line is the result of the fit.
b) $\mathcal{F}(\omega)|V_{cb}|$ as a function of ω. The points are the data, corrected for all detector effects and kinematic terms. The solid line is the result of the fit. The shaded area represents its statistical error and the hatched line its systematic uncertainty.
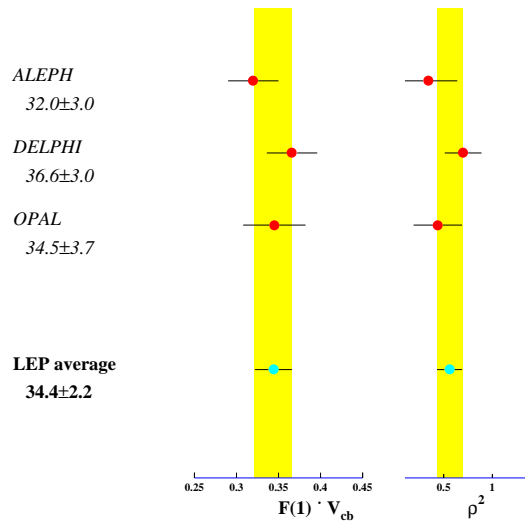

Figure 17: Measurements of $\mathcal{F}(1)|V_{cb}|$ and ρ^2 at LEP.

24

6.1.3 Measurement of proper time t

The proper time from the production to the decay is given by $(t = \frac{l m_B}{c E_B})$, where l is the B-decay length, m_B the B-mass, E_B its energy, and c the speed of light.

l is normally measured from the distance between the fitted primary and secondary vertices. The typical resolution is $\delta l \approx 300 \mu$m compared to a mean decay length of $\langle l \rangle \approx 3$mm. In some of the lepton analyses, instead of the decay length the lepton impact parameter is used, which is on a statistical basis related to the decay length.

The B-energy is measured from the tracks attached to the secondary vertex, the missing energy in the hemisphere, and some correction for photons from the B-decay. Due to the photon correction, the resolution is worse than in the V_{cb}-analyses, typically about 20%.

Figure 18 shows the resolution of the proper time measurement (a) and the resolution normalized to its error (b) for the OPAL $D^{*\pm}\ell$ analysis. Some negative tails due to an imperfect assignment of tracks to the secondary vertex can be observed.

Figure 19 shows the proper time distribution from the ALEPH lepton analysis. The data agree well with the Monte Carlo prediction. All the background is concentrated at small proper times.

6.1.4 Results

To obtain the mixing parameter Δm_d the experiments fit the fraction of mixed events as a function of the proper time. To reduce the systematic uncertainty, apart from Δm_d, some other parameters describing the background and the tagging efficiencies are left free in the fit.

Figure 20 shows the fraction of mixed events from the DELPHI jetcharge-lepton analysis. Good agreement with the fit can be observed. The LEP results are described in [47–50]. All results, including those of CDF and SLD are summarized in figure 21 [46]. The current world average is

$$\Delta m_d = (0.464 \pm 0.012 \pm 0.013)\,\mathrm{ps}^{-1}.$$

6.2 B_s^0-oscillations

The B^0 analyses where a lepton is used to tag the decay charge can also be used to search for a high frequency component in the t-distribution.

In the $D^{*\pm}$ analyses, the $D^{*\pm}$ is replaced by a D_s. This enriches the sample considerably in B_s^0, reducing the statistical error of the analysis.

When a b-quark fragments into a B_s^0 meson there is a high chance that the free s-quark from the fragmentation chain ends up in a Kaon of the same charge as the b-quark. ALEPH has performed an analysis where such a Kaon is used to tag the B_s^0 production charge. However the sensitivity of this analysis is not yet as large as when the production charge is tagged in the opposite hemisphere.

6.2.1 Combination of results

Up to now only lower limits exist for Δm_s. To combine the limits of several analyses inside one experiment, and more of different experiments, the "amplitude method" [51] has been introduced. In this method the oscillation probability is modified to

$$P(B \to \bar{B})(t) = \frac{\Gamma}{2} e^{-\Gamma t}(1 - A \cdot \cos(\Delta m t)).$$

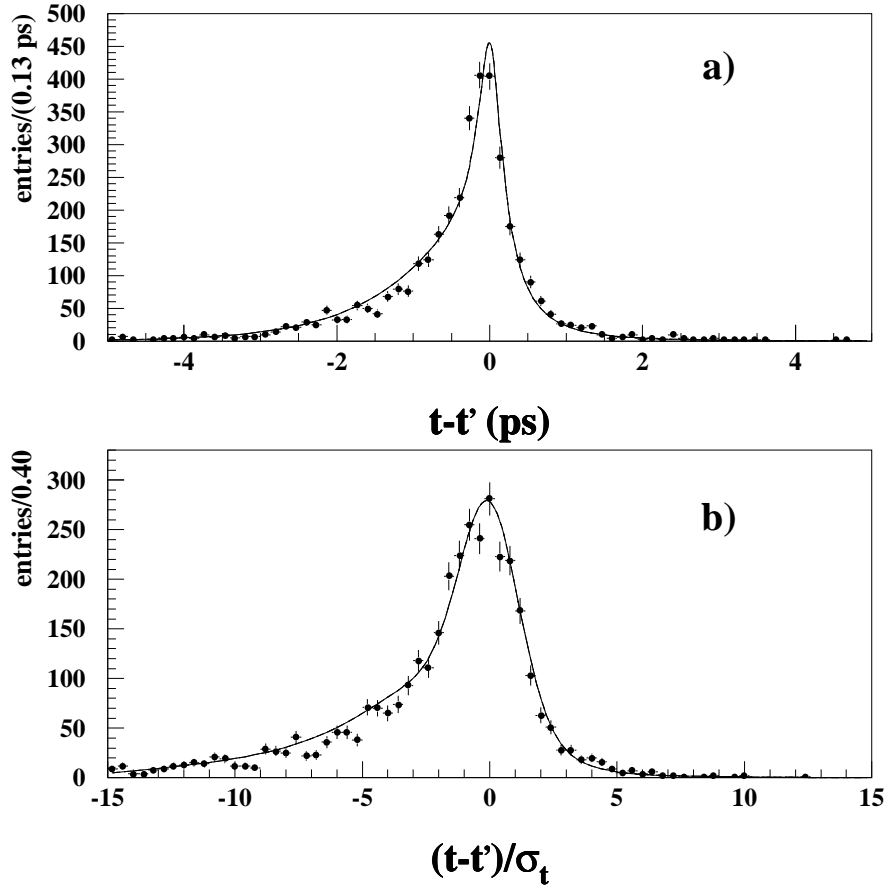Figure 18: a) Difference between the reconstructed proper time t and the true proper time t' in the OPAL D$^{*\pm}\ell$ analysis. The points are the data and the solid line is the prediction from the Monte Carlo.
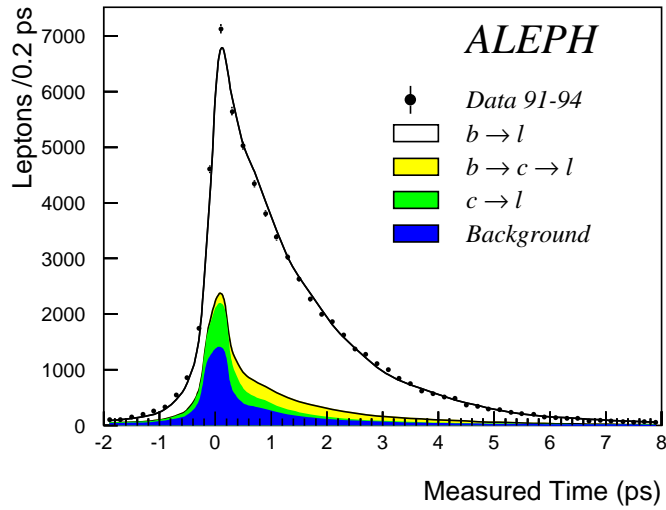b) Same as a) divided by the calculated error on t.

Figure 19: Reconstructed proper time distribution from the ALEPH lepton-jetcharge analysis. The points are the data and the solid line the Monte Carlo prediction. The white area represents the signal and the different shaded areas the background sources.
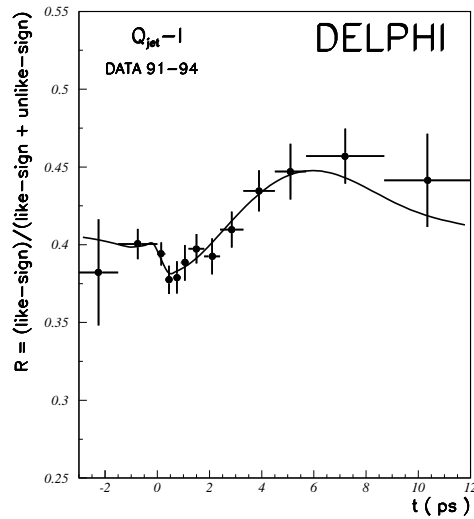
Figure 20: Fraction of mixed events as a function of the reconstructed proper time from the DELPHI lepton-jetcharge analysis.
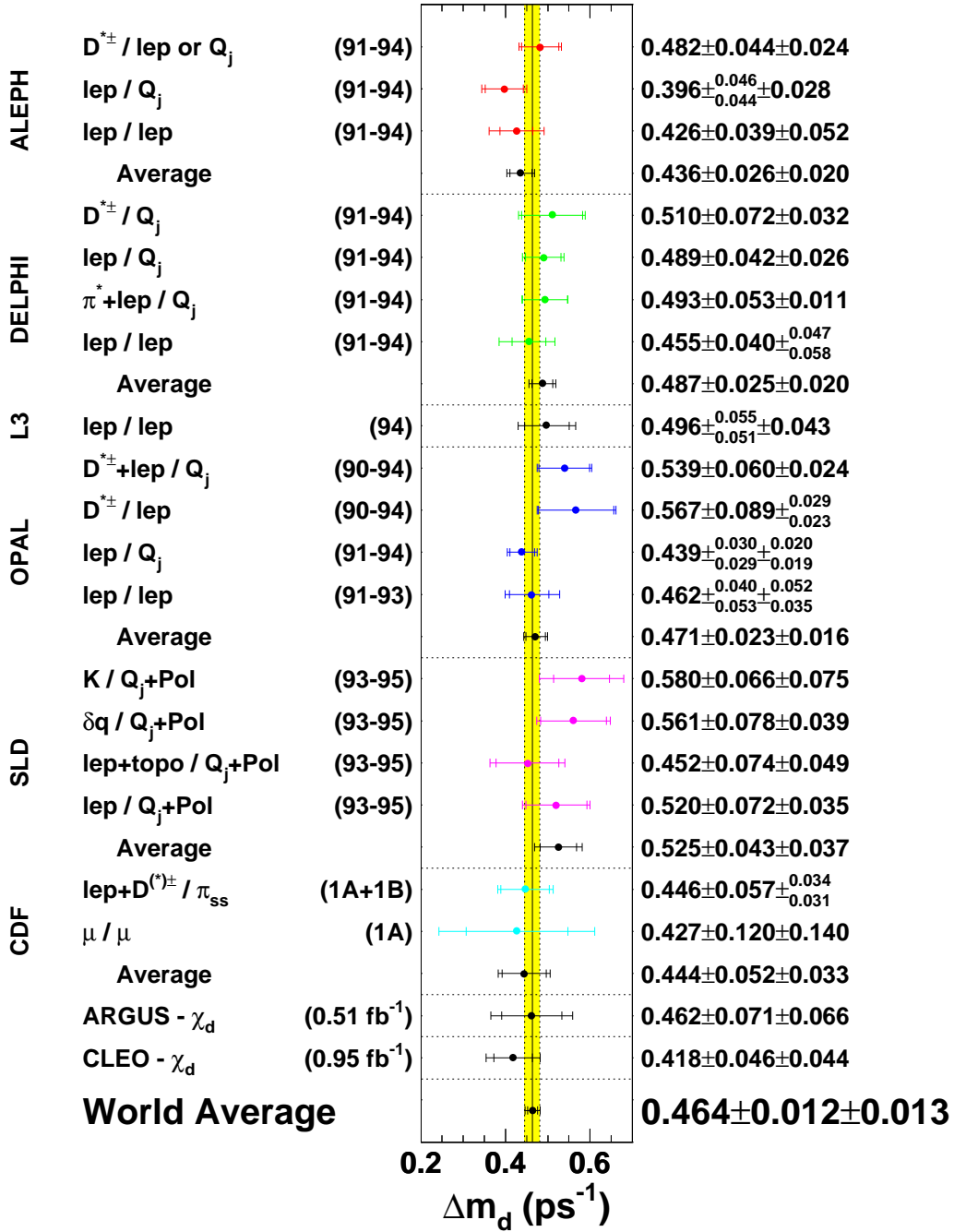
Figure 21: Summary of Δm_d measurements at LEP, SLD and CDF.

In the oscillation fit, Δm is fixed to an arbitrary value and A is fitted instead. If Δm is fixed to the correct value, A has to be compatible with 1. In general $A(\Delta m)$ follows a Breit-Wigner distribution with maximum $A = 1$ in Δm_{true} and width $2/\tau_B$. The assumed Δm can thus be excluded, if the corresponding $A(\Delta m)$ is incompatible with one. To combine several analyses, measurements of A need simply to be combined in the usual way and the compatibility of the combined A with 1 has to be tested. As an example, figure 22 shows the fitted amplitude as a function of Δm_s for the single ALEPH analyses and figure 23 the combined amplitude from ALEPH and DELPHI.
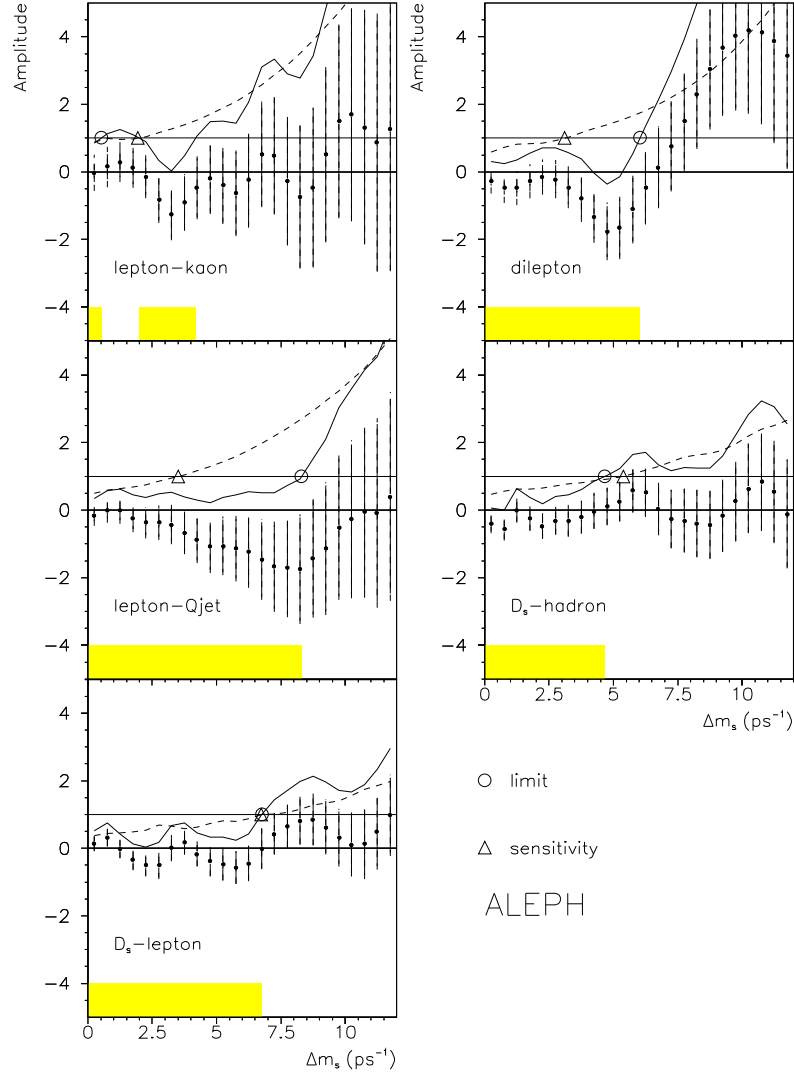

Figure 22: Fitted amplitude A as a function of the assumed Δm_s for the different ALEPH analyses. The points with the error bars are the fitted amplitudes, the solid line the 95% upper limits derived from them and the dashed line the sensitivity, i.e. the upper limit if the central value of the amplitude is put to zero.
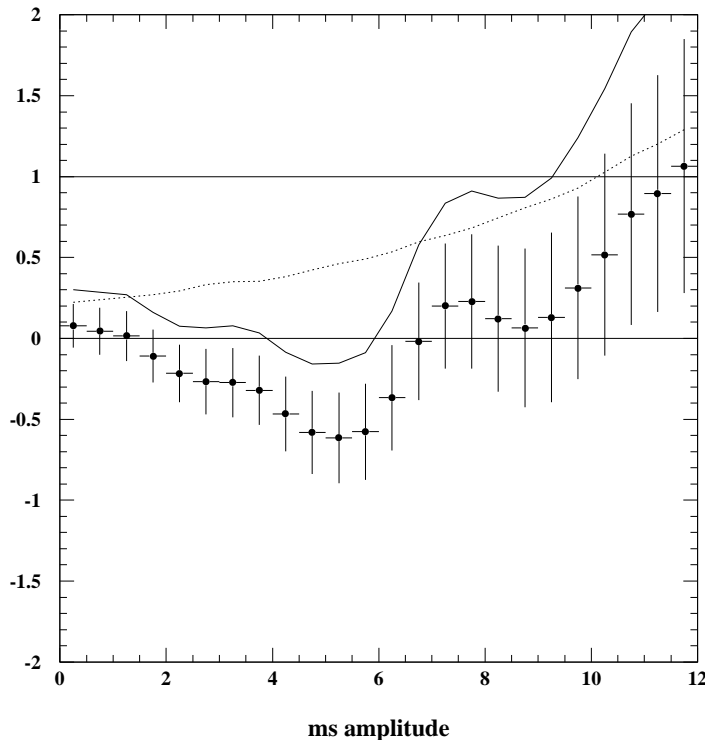
Figure 23: Combined amplitude from ALEPH and DELPHI. The meaning of the points and lines is as in figure 22.

6.2.2 Results

The analyses of ALEPH, DELPHI and OPAL are described in [52–54] and summarized in figure 24. Combining ALEPH and DELPHI results in

$$\Delta m_s < 9.2\mathrm{ps}^{-1} \quad \text{at } 95\% \text{ C.L.}$$

OPAL still used the likelihood method, so their result could not easily be combined with the others.

From figure 24 it can be seen that there is a significant gain from combining experiments. In addition one can see that in the case of ALEPH one analysis has a better exclusion limit than the combination. In fact with about 10 analyses of comparable precision it is quite probable that one of them excludes the true value of Δm_s with 95% C.L.. It is thus wrong to use just the best limit.

7   B-hadron Lifetimes

In the naive spectator model, all b-hadron lifetimes should be equal. It has however been known since long that the lifetimes of charmed hadrons differ up to a factor of three, because of interference effects between the different assignments of decay and spectator quarks to the final state hadrons. Due to the higher b-mass, the lifetime differences in the B-sector are expected to be much smaller.

At LEP all b-hadrons are produced and can be tagged via specific decay modes. The analysis techniques are similar to the ones already described for the V_{cb} analyses and for $B\bar{B}$-mixing. For all hadrons, important updates have been presented this summer.

As an example, figure 25 shows the B^0 lifetime spectrum from a DELPHI analysis with inclusively reconstructed $D^{*\pm}$ [55]. The inclusive reconstruction technique per-
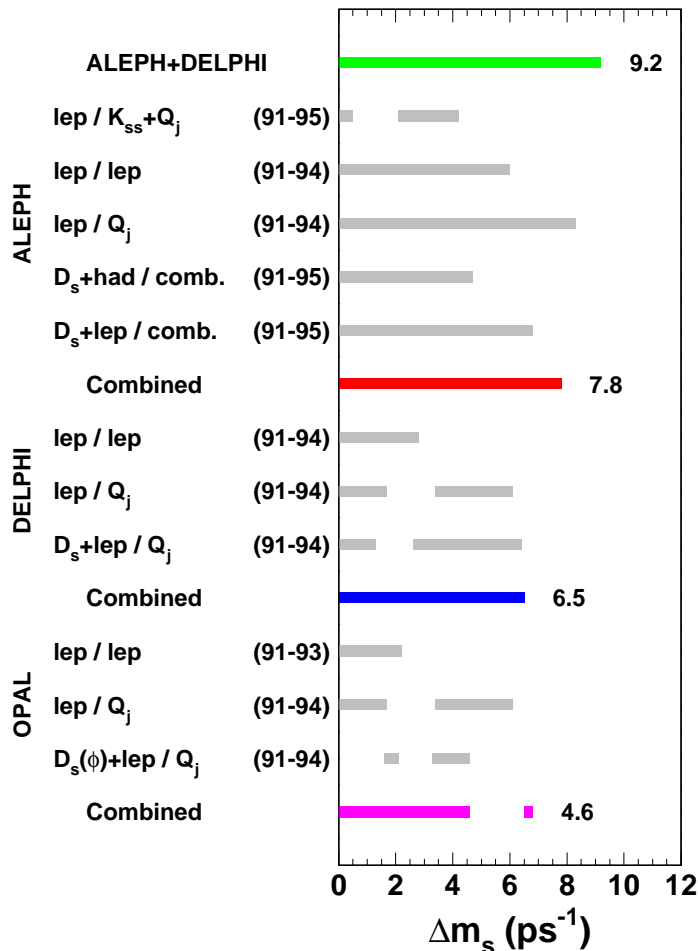
30

Figure 24: Δm_s limits from the different LEP analyses.

mits a high efficiency simultaneously with a high purity and precise estimation of the B-momentum. This analysis obtains about the same precision as the current world average. The results for the different b-hadrons are summarized in tables 8, 9, 10 and 11. The averages have been obtained by the LEP B-lifetime group, taking into account common systematic errors [56]. The B^+, B^0, B^0_s and Λ_b known to 5% or better by now.

Figure 26 compares the ratios of the b-hadron lifetimes to the B^0-lifetime with the theoretical predictions assuming factorization. The ratios of the B-meson lifetimes agree well with the expectation. The lifetime of the b-baryons, however, is about three standard deviations lower than predicted.

8   Conclusions

Using close to the full LEP 1 statistics results on electroweak and heavy flavour physics have been presented. The electroweak results agree on the per mill level with the predictions from the Standard Model. On the heavy flavour sector the production of all B-species and the large boost allows for competitive results with dedicated B-machines.
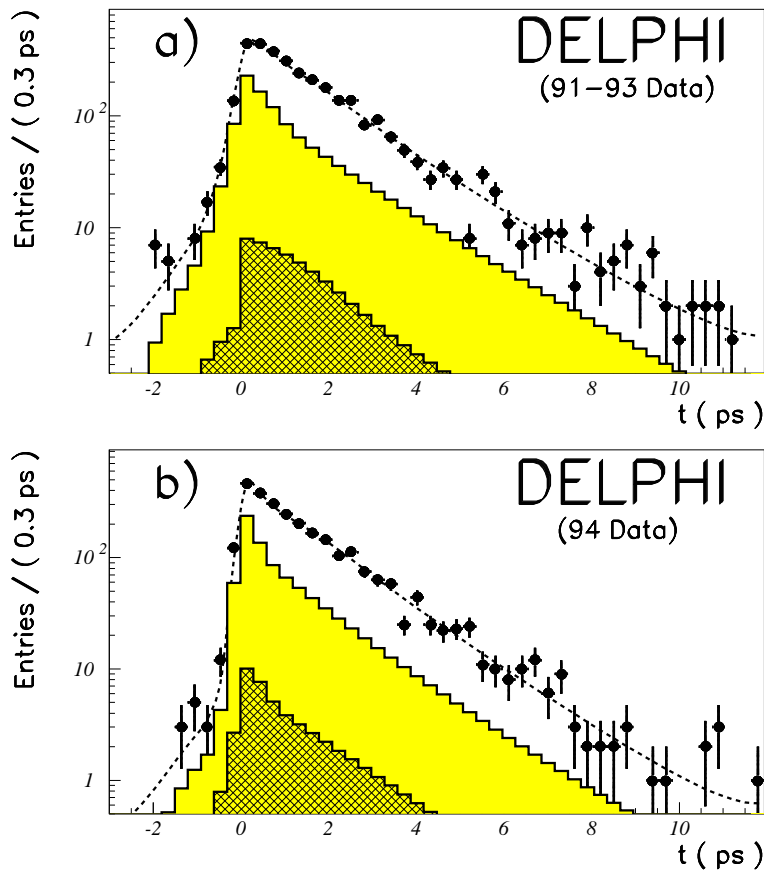
31

Figure 25: Reconstructed proper time distribution from the DELPHI B^0 lifetime analysis. Fig. a) is from the 1991-1993 dataset with a two dimensional silicon vertex detector and b) for the 1994 dataset with an upgraded three dimensional detector. The points are the data, the white area represents the Monte Carlo prediction for the signal and the grey ones are the prediction for the background.

Experiment	Method	Data set	τ_{B^0} (ps)	Reference
ALEPH	$D^{(*)}\ell$	91-94	$1.61\pm0.07\pm0.04$	[57]
ALEPH	Excl. rec.	91-94	$1.25^{+0.15}_{-0.13}\pm0.05$	[57]
ALEPH	Partial rec. $\pi^+\pi^-$	91-94	$1.49^{+0.17+0.08}_{-0.15-0.06}$	[57]
CDF$^{(p)}$	Excl. $(J/\psi K)$	92-93 & 94-95	$1.58\pm0.09\pm0.02$	[58]
CDF	$D^{(*)}\ell$	92-93	$1.54\pm0.08\pm0.06$	[59]
DELPHI	$D^{(*)}\ell$	91-93	$1.61^{+0.14}_{-0.13}\pm0.08$	[60]
DELPHI	Charge sec. vtx.	91-93	$1.63\pm0.14\pm0.13$	[61]
DELPHI	Inclusive $D^*\ell$	91-94	$1.529^{+0.040}_{-0.039}\pm0.039$	[55]
OPAL	$D^{(*)}\ell$	91-93	$1.53\pm0.12\pm0.08$	[62]
SLD$^{(p)}$	Charge sec. vtx.ℓ	93-95	$1.55^{+0.13}_{-0.12}\pm0.09$	[63]
SLD$^{(p)}$	Charge sec. vtx.	93-95	$1.63\pm0.07\pm0.06$	[64]
Average			1.55 ± 0.04	

Table 8: Measurements of B^0 lifetime.(p) preliminary

Experiment	Method	Data set	τ_{B^+} (ps)	Reference
ALEPH	D$^{(*)}\ell$	91-94	$1.58\pm0.09\pm0.04$	[57]
ALEPH	Excl. rec.	91-94	$1.58^{+0.21+0.04}_{-0.18-0.03}$	[57]
CDF$^{(p)}$	Excl. ($J/\psi K$)	92-93 & 94-95	$1.68\pm0.07\pm0.02$	[58]
CDF	D$^{(*)}\ell$	92-93	$1.56\pm0.13\pm0.06$	[59]
DELPHI	D$^{(*)}\ell$	91-93	$1.61\pm0.16\pm0.12$	[60]
DELPHI	Charge sec. vtx.	91-93	$1.72\pm0.08\pm0.06$	[61]
OPAL	D$^{(*)}\ell$	91-93	$1.52\pm0.14\pm0.09$	[62]
SLD$^{(p)}$	Charge sec. vtx. ℓ	93-95	$1.60^{+0.12}_{-0.11}\pm0.06$	[63]
SLD$^{(p)}$	Charge sec. vtx.	93-95	$1.69\pm0.06\pm0.06$	[64]
Average			1.65 ± 0.04	

Table 9: Measurements of B^+ lifetime.(p) preliminary

Experiment	Method	Data set	$\tau_{B^0_s}$ (ps)	Reference
ALEPH	D$_s\ell$	91-95	$1.54^{+0.14}_{-0.13}\pm0.04$	[65]
ALEPH	D$_s h$	91-93	$1.61^{+0.30+0.18}_{-0.29-0.16}$	[66]
CDF$^{(p)}$	D$_s\ell$	92-93 & 94-95	$1.37^{+0.14}_{-0.12}\pm0.04$	[67]
CDF	Excl. $J/\psi\phi$	92-93 & 94-95	$1.34^{+0.23}_{-0.19}\pm0.05$	[68]
DELPHI$^{(p)}$	D$_s\ell$	91-95	$1.53^{+0.17}_{-0.15}\pm0.07$	[69]
DELPHI	D$_s h$	91-94	$1.65^{+0.34}_{-0.31}\pm0.12$	[70]
DELPHI	$\phi\ell$	91-94	$1.76\pm0.20^{+0.15}_{-0.10}$	[70]
DELPHI	D$_s$ inclus.	91-94	$1.60\pm0.26^{+0.13}_{-0.15}$	[70]
OPAL	D$_s\ell$	90-94	$1.54^{+0.25}_{-0.21}\pm0.06$	[71]
Average			1.52 ± 0.07	

Table 10: Measurements of B^0_s lifetime.(p) preliminary

Experiment	Method	Data set	τ_{Λ_b} (ps)	Reference
ALEPH$^{(p)}$	$\Lambda\ell$	91-95	$1.18\pm0.08\pm0.07$	[72]
ALEPH$^{(p)}$	$\Lambda_c\ell$	91-95	$1.21^{+0.13}_{-0.12}\pm0.04$	[72]
ALEPH	$\Xi\ell$	90-95	$1.35^{+0.37+0.15}_{-0.28-0.17}$	[73]
CDF	$\Lambda_c\ell$	92-93 & 94-95	$1.32\pm0.15\pm0.07$	[74]
DELPHI	$\Lambda\ell\pi$ vtx	91-94	$1.46^{+0.22+0.07}_{-0.21-0.09}$	[75]
DELPHI	$\Lambda\mu$ i.p.	91-94	$1.10^{+0.19+0.09}_{-0.17-0.09}$	[75]
DELPHI	$\Lambda_c\ell$	91-94	$1.19^{+0.21+0.07}_{-0.18-0.08}$	[75]
DELPHI	pμ	91-93	$1.27^{+0.35}_{-0.29}\pm0.09$	[76]
DELPHI	$\Xi\ell$	91-93	$1.5^{+0.7}_{-0.4}\pm0.3$	[77]
OPAL	$\Lambda\ell$ i.p.	90-94	$1.21^{+0.15}_{-0.13}\pm0.10$	[78]
OPAL	$\Lambda\ell$ vtx.	90-94	$1.15\pm0.12\pm0.06$	[78]
OPAL	$\Lambda_c\ell$	90-94	$1.14^{+0.22}_{-0.19}\pm0.07$	[79]
Average			1.21 ± 0.06	

Table 11: Measurements of b-baryon lifetime. (p) preliminary
The ALEPH and DELPHI $\Xi\ell$ results are not included in the quoted average since the selected data sample contains mostly Ξ_b while the selected data sample in the other measurements contain mostly Λ_b.
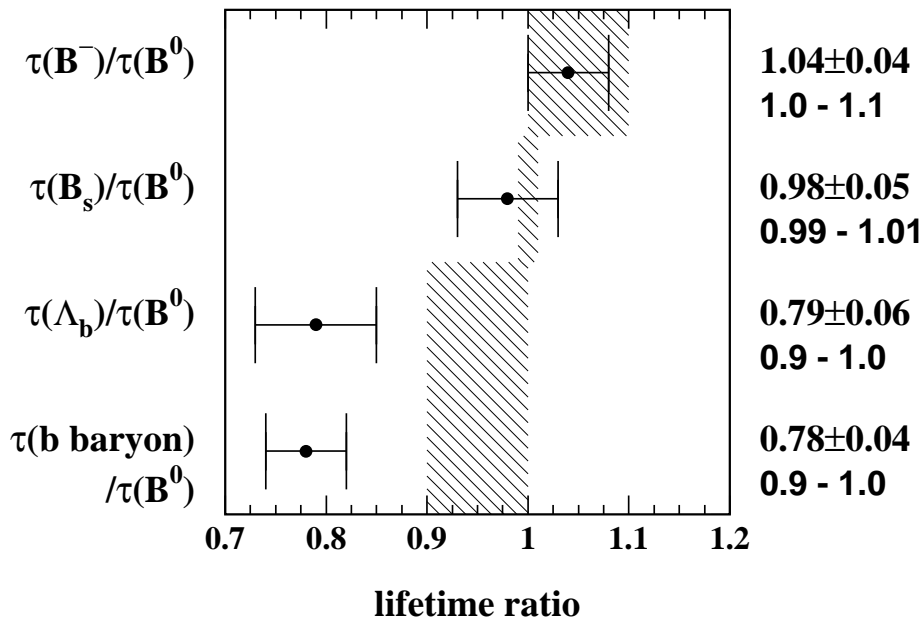
Figure 26: Ratio of the different b-hadron lifetimes to the B^0 lifetime. The points with the error bars are the world averages and the shaded areas the theoretical prediction.

References

[1] G. Wilkinson, *Measurement of the LEP Beam Energy*, talk presented at ICHEP96, Warsaw, 25-31 July 1996, to appear in the proceedings.

[2] ALEPH Collaboration, *Preliminary Results on Z Production Cross Section and Lepton Forward-Backward Asymmetries using the 1990-1995 Data*, contributed paper to ICHEP96, Warsaw, 25-31 July 1996, **PA-07-069**.

[3] DELPHI Collaboration, DELPHI Note 96-118 CONF 65, contributed paper to ICHEP96, Warsaw, 25-31 July 1996, **PA-07-001**.

[4] L3 Collaboration, *Preliminary L3 Results on Electroweak Parameters using 1990-95 Data*, L3 Note 1980, August 1996, available via http://hpl3sn02.cern.ch/note/note-1980.ps.gz.

[5] OPAL Collaboration, *A Preliminary Update of the Z Line Shape and Lepton Asymmetry Measurements with a Revised 1993-1994 LEP Energy and 1995 Lepton Asymmetry*, OPAL Physics Note PN242, July 1996;
OPAL Collaboration, *Measurements of Lepton Pair Asymmetries using the 1995 Data*, contributed paper to ICHEP96, Warsaw, 25-31 July 1996 **PA07-015**.

[6] ALEPH Collaboration, D. Buskulic *et al.*, Zeit. Phys. **C69** (1996) 183.

34

[7] DELPHI Collaboration, P. Abreu *et al.*, Z. Phys. **C67** (1995) 183;
DELPHI Collaboration, *An updated measurement of tau polarisation*, DELPHI 96-114 CONF 42, contributed paper to ICHEP96, Warsaw, 25-31 July 1996, **PA07-008**.

[8] L3 Collaboration, O. Acciari *et al.*, Phys. Lett. **B341** (1994) 245;
L3 Collaboration, *A Preliminary Update of A_τ and A_e Using 1994 Data*, contributed paper to EPS-HEP Brussels, **eps0094**.
The 1994 data have been combined with the earlier data using a 100% correlation of the systematic errors.

[9] OPAL Collaboration, G.Alexander *et al.*, *A Precise Measurement of the Tau Polarization and its Forward-Backward Asymmetry at LEP*, CERN-PPE/96-078, submitted to Z. Phys. C.

[10] S. Willcoq, *Physics at the Z Pole with SLD*, these proceedings.

[11] ALEPH Collaboration, *Measurement of R_b using a Lifetime-Mass Tag*, contributed paper to ICHEP96, Warsaw, 25-31 July 1996 **PA10-014**
ALEPH Collaboration, *A Measurement of R_b using Mutually Exclusive Tags*, contributed paper to ICHEP96, Warsaw, 25-31 July 1996 **PA10-015**.

[12] OPAL Collaboration, R. Akers *et al.*, Z. Phys. **C60** (1993) 199;
OPAL Collaboration, R. Akers *et al.*, *Updated Measurement of the Heavy Quark Forward-Backward Asymmetries and Average B Mixing Using Leptons in Multihadronic Events*, OPAL Physics Note PN226 contributed paper to ICHEP96, Warsaw, 25-31 July 1996 **PA05-007**.

[13] The LEP Experiments: Aleph, Delphi, L3 and Opal, Nucl. Inst. Meth. **A378** (1996) 101.

[14] The LEP heavy flavour group, *Presentation of LEP Electroweak Heavy Flavour Results for Summer 1996 Conferences*, LEPHF/96-01,
available from http://www.cern.ch/LEPEWWG/heavy/

[15] Particle Data Group, M. Barnett *et al.*, Phys. Rev. **D54**(1996) 1.

[16] OPAL Collaboration, R. Akers *et al.*, Phys. Lett. **B353** (1995) 595.

[17] DELPHI Collaboration, *Measurement of Gluon Splitting Probability to Bottom Quark Pairs $g_{b\bar{b}}$ in Hadronic Z^0 Decays*, contributed paper to ICHEP96, Warsaw, 25-31 July 1996 **PA01-035**.

[18] ALEPH Collaboration, D. Buskulic *et al.*, Z. Phys. **C62** (1994) 179;
ALEPH Collaboration, *Measurement of the b forward-backward asymmetries and of the $\bar{\chi}$ mixing parameter using high-p_t leptons*, contributed paper to ICHEP96, Warsaw, 25-31 July 1996 **PA10-002**, CERN-PPE/96-072
ALEPH Collaboration., D. Buskulic *et al.*, *Measurement of the semileptonic b branching ratios from inclusive leptons in Z decays*, Contributed Paper to EPS-HEP-95 Brussels, **eps0404**.

[19] DELPHI Collaboration, P.Abreu *et al.*, Z. Phys **C65** (1995) 569;
DELPHI Collaboration, P.Abreu *et al.*, Z. Phys **C66** (1995) 341;
DELPHI Collaboration, *Measurement of the Forward-Backward Asymmetries of $e^+e^- \to Z \to b\bar{b}$ and $e^+e^- \to Z \to c\bar{c}$*, Contributed Paper to EPS-HEP-95 Brussels, **eps0571**, DELPHI 95-87 PHYS 522.

[20] L3 Collaboration, *L3 Results on A^b_{FB}, A^c_{FB} and χ for the Glasgow Conference*, L3 Note 1624;
L3 Collaboration, *L3 Results on R_b and Br(b $\to \ell$) for the Glasgow Conference*, L3 Note 1625.

The sign of the correlation coefficient arising from the b semileptonic decay model has been corrected.

[21] OPAL Collaboration, R. Akers *et al.*, Z. Phys. **C60** (1993) 199;
OPAL Collaboration, R. Akers *et al.*, *Updated Measurement of the Heavy Quark Forward-Backward Asymmetries and Average B Mixing Using Leptons in Multi-hadronic Events*, OPAL Physics Note PN226 contributed paper to ICHEP96, Warsaw, 25-31 July 1996 **PA05-007**.

[22] ALEPH Collaboration, D. Buskulic *et al.*, Phys. Lett. **B335** (1994) 99.
ALEPH Collaboration, *An Upgraded Measurement of $A_{\rm FB}^{\rm b}$ from the charge asymmetry in Lifetime Tagged Z Decays*, contributed paper to ICHEP96, Warsaw, 25-31 July 1996 **PA10-018**.

[23] OPAL Collaboration, R. Akers *et al.*, Z. Phys. **C67** (1995) 365.

[24] ALEPH Collaboration, D. Buskulic *et al.*, Z. Phys. **C62** (1994) 1;
ALEPH Collaboration, D. Buskulic *et al.*, *The Forward–Backward Asymmetry for Charm Quarks at the Z pole: an Update*, contributed paper to EPS-HEP-95 Brussels, **eps0634**.

[25] OPAL Collaboration, *A Measurement of the Charm and Bottom Forward-Backward Asymmetry using D Mesons with the OPAL Detector at LEP*, contributed paper to EPS-HEP-95 Brussels, **eps0290**, OPAL Physics Note, PN183.

[26] ALEPH Collaboration, *Measurement of the partial decay width of the Z into $c\bar{c}$ quarks*, contributed paper to ICHEP96, Warsaw, 25-31 July 1996 **PA10-016**.

[27] DELPHI Collaboration, *Summary of R_c measurements in DELPHI,* DELPHI 96-110 CONF 37 contributed paper to ICHEP96, Warsaw, 25-31 July 1996 **PA01-060**.

[28] OPAL Collaboration, R. Akers *et al.*, Z. Phys. **C67** (1995) 27;
OPAL collaboration, CERN-PPE/96-51 12 April 1996;
OPAL Collaboration, *A measurement of $BR({\rm c} \to {\rm D}^*)$ and $\Gamma_{\rm c\bar{c}}/\Gamma_{had}$ using a double tagging method*, OPAL Physics Note PN227 contributed paper to ICHEP96, Warsaw, 25-31 July 1996 **PA05-011**.

[29] DELPHI Collaboration, P.Abreu *et al.*, Z. Phys. **C70** (1996) 531.
DELPHI Collaboration, P. Abreu *et al.*, *Measurement of the partial decay width $R_b = \Gamma_{b\bar{b}}/\Gamma_{had}$ with the DELPHI detector at LEP*, contributed paper to ICHEP96, Warsaw, 25-31 July 1996 **PA10-061**.

[30] L3 Collaboration, *Measurement of the Z Branching Fraction into Bottom Quarks Using Lifetime Tags*, contributed paper to ICHEP96, Warsaw, 25-31 July 1996 **PA05-049**.

[31] OPAL Collaboration, Z. Phys. **C65** (1995) 17-30;
An Update of the Measurement of $\Gamma_{b\bar{b}}/\Gamma_{had}$ using a Double Tagging Method, contributed paper to EPS-HEP-95 Brussels, **eps0278**, OPAL Physics Note PN181.

[32] G. Altarelli and R. Barbieri, Phys. Lett. **B253** (1991) 161;
G. Altarelli, R. Barbieri and S. Jadach, Nucl. Phys. **B369** (1992) 3;
G. Altarelli, R. Barbieri and F. Caravaglios, Nucl. Phys. **B405** (1993) 3.

[33] D. Bardin *et al.*, Z. Phys. **C44** (1989) 493; Comp. Phys. Comm. **59** (1990) 303; Nucl. Phys. **B351**(1991) 1; Phys. Lett. **B255** (1991) 290 and CERN-TH 6443/92 (May 1992).

[34] *Reports of the working group on precision calculations for the Z resonance*, eds. D. Bardin, W. Hollik and G. Passarino, CERN Yellow Report 95-03, Geneva, 31 March 1995.

[35] Electroweak libraries used:
ZFITTER: see Reference [33];
BHM: G. Burgers, W. Hollik and M. Martinez; M. Consoli, W. Hollik and F. Jegerlehner, *Proceedings of the Workshop on Z physics at LEP I*, CERN Report 89-08 Vol.I, 7; G. Burgers, F. Jegerlehner, B. Kniehl and J. Kühn, the same proceedings, CERN Report 89-08 Vol.I, 55.
These computer codes have been upgraded recently by including the results of [34] and references therein.

[36] M. Paulini *Heavy Flavour Physics – from Top to Bottom*, these proceedings.

[37] C. Klophenstein *Electroweak Tests and Searches for New Phenomena from the Tevatron*, these proceedings.

[38] CDHS Collaboration, H. Abramowicz *et al.*, Phys. Rev. Lett. **57** (1986) 298;
CDHS Collaboration, A. Blondel *et al.*, Z. Phys. **C45** (1990) 361.

[39] CHARM Collaboration, J.V. Allaby *et al.*, Phys. Lett. **B177** (1986) 446;
CHARM Collaboration, J.V. Allaby *et al.*, Z. Phys.**C36** (1987) 611.

[40] CCFR Collaboration, C.G. Arroyo *et al.*, Phys. Rev. Lett. **72** (1994) 3452.

[41] I. Caprini, M. Neubert, Phys. Lett. **B380** (1996) 376

[42] ALEPH Collaboration *Measurements of $|V_{cb}|$ and form factors and branching ratios of $B^0 \rightarrow D^{*+}\ell^-\nu$ and $B^0 \rightarrow D^+\ell^-\nu$*, contributed paper to ICHEP96, Warsaw, 25-31 July 1996 **PA05-056**.

[43] DELPHI Collaboration, P. Abreu *et al.*, Zeit. Phys. **C71** (1996) 539

[44] OPAL Collaboration, *A Measurement of $|V_{cb}|$ Using $B^0 \rightarrow D^{*+}\ell^-\nu$ Decays*, contributed paper to ICHEP96, Warsaw, 25-31 July 1996 **PA08-008**.

[45] M. Margoni, Talk given at the XXVIII International Conference on High Energy Physics, 25-31 July 96, Warsaw, Poland.

[46] L. Gibbons, Plenary talk given at the XXVIII International Conference on High Energy Physics, 25-31 July 96, Warsaw, Poland.

[47] ALEPH Collab *Improved measurement of the $B_d^0\bar{B}_d^0$ oscillation frequency*, contributed paper to ICHEP96, Warsaw, 25-31 July 1996 **PA05-055**.

[48] DELPHI Collab *Measurement of $B_d^0\bar{B}_d^0$ oscillations*, contributed paper to ICHEP96, Warsaw, 25-31 July 1996 **PA01-038**. ICHEP-96 PA01-038,

[49] L3 Collaboration, *Measurement of the B_d^0 Meson Oscillation Frequency using Dilepton Events with the L3 Detector*, contributed paper to ICHEP96, Warsaw, 25-31 July 1996 **PA05-048**.

[50] OPAL Collaboration, *A Study of B Meson Oscillations Using Inclusive Lepton Events*, ICHEP-96 PA08-011,
OPAL Collaboration, G. Alexander *et al.*, *A Measurement of the B_d^0 Oscillation Frequency Using Leptons and $D^{*\pm}$ Mesons*, CERN–PPE/96–74, Submitted to Zeit. Phys. **C**
OPAL Collaboration, R. Akers *et al.*, Zeit. Phys. **C66** (1995) 555.

[51] H.G. Moser, A. Roussarie, *Mathematical methods for for $B^0\bar{B}^0$ oscillation analyses*, Subm. to Nucl. Inst. Meth.

[52] ALEPH Collab *Combined limit on the B_s^0 oscillation frequency*, contributed paper to ICHEP96, Warsaw, 25-31 July 1996 **PA08-020**.

[53] DELPHI Collab *Search for $B_s^0\bar{B}_s^0$ oscillations*, contributed paper to ICHEP96, Warsaw, 25-31 July 1996 **PA01-039**.

[54] OPAL Collab *OPAL combined study of B_s oscillations*, contributed paper to ICHEP96, Warsaw, 25-31 July 1996 **PA08-010**.

[55] DELPHI Collaboration, *Accurate measurement of the B_d^0 meson lifetime*, contributed paper to ICHEP96, Warsaw, 25-31 July 1996 **PA01-041**.

[56] The LEP B lifetimes working group, *Averaging Lifetimes for B Hadron Species*, The LEP B lifetimes working group, *Averages of B Hadron Lifetimes*, available from http://wwwcn.cern.ch/ claires/lepblife.html

[57] ALEPH Collaboration, D. Buskulic *et al.*, Zeit Phys. **C71** (1996) 31

[58] CDF Collaboration, http://www-cdf.fnal.gov/physics/new/bottom/bottom.html

[59] CDF Collaboration, F. Abe *et al.*, Phys. Rev. Lett. **76**, (1996) 4462.

[60] DELPHI Collaboration, P. Abreu *et al.*, Zeit. Phys. **C68** (1995) 13

[61] DELPHI Collaboration, W. Adam *et al.*, Zeit. Phys. **C68** (1995) 363

[62] OPAL Collaboration, R. Akers *et al.*, Zeit. Phys. **C67** (1995) 379

[63] SLD Collaboration, *Measurement of the B^+ and B^0 Lifetimes from Semileptonic Decays at SLD*, contributed paper to ICHEP96, Warsaw, 25-31 July 1996 **PA05-084**.

[64] SLD Collaboration, *Measurement of the B^+ and B^0 Lifetimes with topological vertexing at SLD*, contributed paper to ICHEP96, Warsaw, 25-31 July 1996 **PA05-085**.

[65] ALEPH Collaboration, D. Buskulic *et al.*, Phys. Lett. **B377** (1996) 205

[66] ALEPH Collaboration, D. Buskulic *et al.*, Zeit. Phys. **C69** (1996) 585

[67] CDF Collaboration, *Measurement of the Lifetime of the B_s^0 Meson from $D_s\ell$ Correlation*, contributed paper to ICHEP96, Warsaw, 25-31 July 1996 **PA05-098d**.

[68] CDF Collaboration, F. Abe *et al.*, Phys. Rev. Lett. **77** (1996) 1945

[69] DELPHI Collaboration, *Mean lifetime of the B_s^0 meson*, contributed paper to ICHEP96, Warsaw, 25-31 July 1996 **PA01-042**.

[70] DELPHI Collaboration, P. Abreu *et al.*, Zeit. Phys. **C71** (1996) 11

[71] OPAL Collaboration, R. Akers *et al.*, Phys. Lett. **B350** (1995) 273

[72] ALEPH Collaboration, *Updated Measurement of the b Baryon Lifetime*, contributed paper to ICHEP96, Warsaw, 25-31 July 1996 **PA01-068**.

[73] ALEPH Collaboration, D. Buskulic *et al.*, CERN-PPE/96-081, Submitted to Phys. Lett. **B**

[74] CDF Collaboration, F. Abe *et al.*, Phys. Rev. Lett. **77** (1996) 1439

[75] DELPHI Collaboration, P. Abreu *et al.*, Zeit. Phys. **C71** (1996) 199

[76] DELPHI Collaboration, P. Abreu *et al.*, Zeit. Phys. **C68** (1995) 375

[77] DELPHI Collaboration, P. Abreu *et al.*, Zeit. Phys. **C68** (1995) 541

[78] OPAL Collaboration, R. Akers *et al.*, Zeit. Phys. **C69** (1996) 195

[79] OPAL Collaboration, R. Akers *et al.*, Phys. Lett. **B353** (1995) 402